Free Radical Biology and Medicine 115 (2018) 202–218

Contents lists available at ScienceDirect

Free Radical Biology and Medicine

journal homepage: www.elsevier.com/locate/freeradbiomed

KRIT1 loss-of-function induces a chronic Nrf2-mediated adaptive homeostasis that sensitizes cells to oxidative stress: Implication for Cerebral Cavernous Malformation disease

Cinzia Antognelli[a,*,1,2], Eliana Trapani[b,1,2], Simona Delle Monache[c,2], Andrea Perrelli[b,2], Martina Daga[b,2], Stefania Pizzimenti[b,2], Giuseppina Barrera[b,2], Paola Cassoni[d,2], Adriano Angelucci[c,2], Lorenza Trabalzini[e,2], Vincenzo Nicola Talesa[a,2], Luca Goitre[b,2], Saverio Francesco Retta[b,*,2]

[a] Department of Experimental Medicine, University of Perugia, Italy
[b] Department of Clinical and Biological Sciences, University of Torino, Regione Gonzole 10, Orbassano, 10043 Torino, Italy
[c] Department of Biotechnological and Applied Clinical Science, University of L'Aquila, Italy
[d] Department of Medical Sciences, University of Torino, Italy
[e] Department of Biotechnology, Chemistry and Pharmacy, University of Siena, Italy

ARTICLE INFO

Keywords:
Cerebrovascular disease
Cerebral Cavernous Malformations
CCM1/KRIT1
Oxidative stress
Antioxidant defense
Adaptive redox homeostasis
Redox signaling
Nuclear factor erythroid 2-related factor 2 (Nrf2)
c-Jun
Glyoxalase 1 (Glo1)
Heme oxygenase-1 (HO-1)
Argpyrimidine-modified heat-shock proteins
Oxidative DNA damage and apoptosis

ABSTRACT

KRIT1 (*CCM1*) is a disease gene responsible for Cerebral Cavernous Malformations (CCM), a major cerebrovascular disease of proven genetic origin affecting 0.3–0.5% of the population.

Previously, we demonstrated that KRIT1 loss-of-function is associated with altered redox homeostasis and abnormal activation of the redox-sensitive transcription factor c-Jun, which collectively result in pro-oxidative, pro-inflammatory and pro-angiogenic effects, suggesting a novel pathogenic mechanism for CCM disease and raising the possibility that KRIT1 loss-of-function exerts pleiotropic effects on multiple redox-sensitive mechanisms.

To address this possibility, we investigated major redox-sensitive pathways and enzymatic systems that play critical roles in fundamental cytoprotective mechanisms of adaptive responses to oxidative stress, including the master Nrf2 antioxidant defense pathway and its downstream target Glyoxalase 1 (Glo1), a pivotal stress-responsive defense enzyme involved in cellular protection against glycative and oxidative stress through the metabolism of methylglyoxal (MG). This is a potent post-translational protein modifier that may either contribute to increased oxidative molecular damage and cellular susceptibility to apoptosis, or enhance the activity of major apoptosis-protective proteins, including heat shock proteins (Hsps), promoting cell survival.

Experimental outcomes showed that KRIT1 loss-of-function induces a redox-sensitive sustained upregulation of Nrf2 and Glo1, and a drop in intracellular levels of MG-modified Hsp70 and Hsp27 proteins, leading to a chronic adaptive redox homeostasis that counteracts intrinsic oxidative stress but increases susceptibility to oxidative DNA damage and apoptosis, sensitizing cells to further oxidative challenges. While supporting and extending the pleiotropic functions of KRIT1, these findings shed new light on the mechanistic relationship between KRIT1 loss-of-function and enhanced cell predisposition to oxidative damage, thus providing valuable new insights into CCM pathogenesis and novel options for the development of preventive and therapeutic strategies.

Abbreviations: AGEs, advanced glycation end-products; ARE, antioxidant-response element; AP, argpyrimidine (Nδ-(5-hydroxy-4,6-dimethylpyrimidine-2-yl)-l-ornithine); BBB, blood-brain barrier; Casp-3, Caspase-3; CCM, Cerebral Cavernous Malformation; CNS, central nervous system; COX-2, cycloxygenase-2; Cyt c, cytochrome c; EndMT, endothelial-to-mesenchymal transition; Glo1, Glyoxalase 1; hBMEC, human brain microvascular endothelial cells; HO-1, Heme oxygenase-1; Hsp, heat-shock protein; ICH, intracerebral hemorrhage; JNK, c-Jun NH2-terminal kinase; Keap1, Kelch-like ECH-associated protein 1; KRIT1, Krev interaction trapped 1; MEF, mouse embryonic fibroblast; MG, methylglyoxal; Nrf2, nuclear factor erythroid 2-related factor 2; NVU, neurovascular unit; PTM, post-translational modification; ROS, reactive oxygen species; SOD, superoxide dismutase; TUNEL, TdT-mediated dUTP nick-end labeling

* Corresponding authors.
E-mail addresses: cinzia.antognelli@unipg.it (C. Antognelli), francesco.retta@unito.it (S.F. Retta).
[1] These authors contributed equally to this work.
[2] CCM Italia research network (www.ccmitalia.unito.it).

https://doi.org/10.1016/j.freeradbiomed.2017.11.014
Received 26 March 2017; Received in revised form 18 October 2017; Accepted 15 November 2017
Available online 21 November 2017

1. Introduction

Cerebral cavernous malformation (CCM), also known as cavernous angioma or cavernoma, is a major vascular dysplasia occurring mainly within the central nervous system (CNS) and consisting of closely clustered, abnormally dilated and leaky capillaries [1,2]. CCM lesions have a prevalence of 0.3–0.5% in the general population and can appear as single or multiple (up to hundreds) mulberry-like vascular sinusoids of varying size, lined by a thin endothelium devoid of normal vessel structural components, such as pericytes and astrocyte end-feet. They can remain asymptomatic throughout life or result in clinical symptoms of various type and severity at any age, including recurrent headaches, focal neurological deficits, seizures, stroke and intracerebral hemorrhage (ICH) [1–3].

This cerebrovascular disease is of proven genetic origin, and may arise sporadically or is inherited as autosomal dominant condition with incomplete penetrance and highly variable expressivity, including wide inter-individual differences in lesion number, size and susceptibility to ICH even among family members of similar ages carrying the same disease-associated genetic defect [4]. Genetic studies have identified three disease genes, *KRIT1* (also known as *CCM1*), *CCM2* and *PDCD10* (also known as *CCM3*) [5], whose functions need to be severely impaired for pathogenesis. Indeed, most of the more than one hundred distinct causative mutations identified so far in these genes are loss-of-function mutations. In particular, mutations of the *KRIT1* gene account for over 50% of familial cases (up to 70% in Hispanic Americans) [5]. This gene encodes for a 736 amino acid protein that has been implicated in the maintenance of endothelial cell-cell junction stability and blood-brain barrier (BBB) integrity through the regulation of major cell structures and signaling mechanisms, including cadherin-mediated cell-cell junctions [6], integrin-mediated cell-matrix adhesion [7,8], Rho GTPase-mediated cytoskeleton dynamics [9,10], and TGFβ-driven endothelial-to-mesenchymal transition (EndMT) [11]. In addition, in recent years it has become clear that KRIT1 plays an important role in controlling signaling pathways involved in cell responses to oxidative stress and inflammatory events [12–21]. In particular, original findings demonstrated that KRIT1 loss-of-function is associated with increased intracellular levels of reactive oxygen species (ROS) and enhanced cell susceptibility to oxidative stress-mediated molecular dysfunctions and oxidative damage [15]. Moreover, subsequent findings showed that KRIT1 may exert a protective role against oxidative stress by limiting c-Jun-dependent redox pathways [16] and defective autophagy [18–20]. Accordingly, recent evidence in animal models has suggested that oxidative stress is linked to the pathogenesis of CCM disease and may play an even more critical role than previously described due to systemic effects [14]. Furthermore, growing data in cellular and animal models indicate that limiting ROS accumulation and oxidative stress via distinct approaches may contribute significantly in preventing or reversing CCM disease phenotypes [14,16–18,20,22].

Despite the significant progress in understanding CCM pathogenesis, no direct therapeutic approaches for CCM disease exist so far other than the surgical removal of accessible lesions in patients with recurrent hemorrhage or intractable seizures [3]. Moreover, specific pharmacological strategies are also required for preventing the *de novo* formation of CCM lesions and counteracting disease progression and severity in susceptible individuals, including CCM gene mutation carriers. Indeed, while the great advances in knowledge of physiopathological functions of CCM proteins have led to an explosion of disease-relevant molecular information, they have also clearly indicated that loss-of-function of these proteins has potentially pleiotropic effects on several biological pathways, thus bringing new research challenges for a more comprehensive understanding [20,21]. In particular, further investigation into the emerging role of KRIT1 in redox-sensitive pathways and mechanisms is required to gain a better understanding of the likely complex signaling networks underlying the physiopathological functions of this important protein, thus facilitating the development of novel strategies for CCM disease prevention and treatment.

A fundamental mechanism that governs cellular adaptive defense against endogenous and exogenous oxidative stress is the activation of the redox-sensitive transcription factor Nrf2 (nuclear factor erythroid 2-related factor 2), which controls constitutive and inducible expression of a plethora of antioxidant responsive element (ARE)-driven genes involved in detoxification of reactive oxidants and maintenance of cellular homeostasis [23–25]. Nrf2 is in fact the master regulator of cytoprotective responses to counteract oxidative and electrophilic stress through the coordinated induction of major antioxidant and phase II detoxification enzymes. These cytoprotective pathways may in turn prevent apoptosis and enhance cell survival by attenuating oxidative damage, mitochondrial dysfunction, and inflammation, and increasing cellular defense and repair mechanisms, thus playing a critical role in protection against various diseases, including vascular diseases [25,26]. In particular, activation of the essential Nrf2/ARE antioxidant defense pathway and its key downstream target heme oxygenase-1 (HO-1) within the neurovascular unit (NVU) has been shown to protect the cerebral vasculature against oxidative stress-mediated BBB breakdown and inflammation in stroke [27,28].

Besides HO-1, Glyoxalase 1 (Glo1) is emerging among the major downstream targets of Nrf2 transcriptional activity as a crucial stress-responsive defense protein for cellular protection against both dicarbonyl glycation and oxidative stress [29]. Glo1 is an ubiquitous glutathione-dependent enzyme that plays a critical cytoprotective role in limiting intracellular accumulation and toxicity of methylglyoxal (MG), a highly reactive dicarbonyl compound that is inevitably formed as a by-product of metabolic pathways, such as glycolysis [30]. MG readily reacts with lipids, nucleic acids and proteins (particularly with nucleophilic groups on side chains of Arg, Lys and Cys residues) to form the heterogeneous family of advanced glycation end-products (AGEs) [31,32]. MG-derived dicarbonyl adducts exert complex pleiotropic effects on normal and pathologic processes in cells, including modulation of protein biological activity [33] and stability [34], and generation of ROS and oxidative stress [35,36], which may culminate in distinct biological outcomes [36–41]. In particular, supra-physiological accumulation of argpyrimidine (AP), a major AGE formed by spontaneous reaction between MG and protein arginine residues [40], has been shown to induce oxidative DNA damage and apoptosis [39–42]. However, post-translational modifications (PTM) by MG-derived AP can also enhance the functionality of fundamental stress-inducible proteins implicated in cellular recovery after exposure to damaging stimuli and protection against apoptosis, including heat shock protein 27 (Hsp27), thus playing an important role in cell survival [43,44]. Furthermore, there is also evidence that some MG-derived AGEs, including AP, are endowed with antioxidant properties [45]. These apparently divergent functions imply that MG, like other reactive species, may exert different or even opposite biological effects, depending on its levels and the cellular context. Interestingly, Glo1 and MG-derived AGEs have been shown to play major and complex roles in vascular physiology and pathophysiology, including the pathogenesis of brain microvascular endothelial barrier dysfunctions [46–48].

The present study was designed to assess the putative involvement of major regulators of cellular responses to oxidative stress, including Nrf2 and Glo1, in the emerging relationship between KRIT1 loss-of-function and enhanced cell sensitivity to oxidative challenges [21].

2. Materials and methods

2.1. Cell culture and treatment

KRIT1$^{-/-}$ and KRIT1$^{+/+}$ mouse embryonic fibroblast (MEF) cell lines were established from KRIT1$^{-/-}$ and KRIT1$^{+/+}$ E8.5 mouse embryos, respectively, whereas KRIT1 9/6 MEFs were obtained by infecting KRIT1$^{-/-}$ cells with a lentiviral vector encoding KRIT1 [15]. Cells were cultured at 37 °C and 5% CO_2 in Dulbecco's modified Eagle's medium

(DMEM) supplemented with 10% fetal calf serum (FCS), 2 mM glutamine, and 100 U/ml penicillin/streptomycin.

The human brain microvascular endothelial cells (hBMEC) were purchased from ScienCell Research Laboratory (Carlsbad, CA), and cultured at 37 °C and 5% CO_2 on cell culture dishes coated with rat tail collagen type-I (BD Biosciences, San Jose, CA) and containing EGM-2MV medium (Lonza, Basel, Switzerland), following manufacturer's instructions.

Cells grown in complete culture medium were either mock-treated or treated with specific compounds, including the mitochondria-permeable superoxide dismutase (SOD) mimetic Tiron (4,5-dihydroxy-1,3-benzenedisulfonic acid disodium salt monohydrate, Sigma-Aldrich, Milan, Italy) (5 mM for 24 h), the JNK inhibitor SP600125 (Calbiochem-Merck, Darmstadt, Germany) (25 μM for 1 h) [16], and the autophagy inducer Rapamycin (Calbiochem) (500 nM for 4 h) [18]. The given concentrations of these compounds were based on the outcomes of previous works [16,18] and preliminary optimization experiments, showing no significant toxicity to cells and optimal efficacy in specific biochemical assays.

2.2. Cell transfection and siRNA-mediated gene silencing

For small interfering RNA (siRNA)-mediated KRIT1 knockdown, hBMEC cells were subjected to a two-round transfection procedure with a mix of four pre-designed iBONi siRNAs targeting KRIT1 (D-00101-Plus, Ribbox GmbH, Germany) or an iBONi siRNA negative control (K-00301-0005-N3, Ribbox GmbH), as previously described [18]. Briefly, 18–24 h before transfection, cells were plated at a density of 2×10^5 cells/well in a 6-well plate with 2.5 ml complete EGM-2MV medium per well, and reached 50–70% confluence at the time of transfection. The transfection complex was prepared by mixing 25 nM iBONi siRNAs and 1:166 HiPerFect reagent (Qiagen, Milan, Italy) in serum-free growth medium and incubating at room temperature for 15 min, and added dropwise to the 6-well plates containing cells in complete growth medium. Upon overnight incubation in the transfection mix, cells were washed and fed with complete EGM-2MV medium. The siRNA transfection procedure was repeated after 48 h to obtain a higher degree of knockdown; then cells were seeded into assay plates and subjected to experimental conditions within 48–72 h. The KRIT1 knockdown efficiency was monitored by quantitative real-time polymerase chain reaction (qRT-PCR) and Western blotting (WB) analysis.

siRNA-mediated knockdown of Glo1 was performed as described in [49].

2.3. RNA isolation, reverse transcription, and quantitative real time PCR analysis (qRT-PCR)

Total cellular RNA was isolated using TRIzol Reagent (Invitrogen, Milan, Italy). cDNA was then synthesized from 1 μg of RNA using the RevertAid™ H Minus First Strand cDNA Synthesis Kit (Carlo Erba, Milan, Italy). To quantify transcript expression levels, an optimal Sybr Green or TaqMan real-time PCR assay was designed for Glo1 or the appropriate housekeeping genes, using Beacon Designer 4 software (Stratagene), starting from published sequence data supplied by the NCBI database. Sybr Green or TaqMan gene expression was performed in triplicate on a MX3000 P Real-Time PCR System (Agilent Technology, Milan, Italy). The sequences of oligonucleotide primers and TaqMan probes used were as follows: Mus musculus Glo1: 5′-acgacagacaaagccacctgattg-3′ (sense, 400 nM), 5′-agcccaagtgtgagcagagagc-3′ (antisense, 400 nM); Mus musculus KLF2: 5′-cgcctcgggttcatttc-3′ (sense, 600 nM), 5′-agcctatcttgccgtccttt-3′ (antisense, 600 nM); Mus musculus KLF4: 5′-gtgccccgactaaccgttg-3′ (sense, 600 nM), 5′-gtcgttgaactcctcggtct-3′ (antisense, 600 nM); Mus musculus GAPDH: 5′-ccaatgtgtccgtcgtggat-3′ (sense, 600 nM), 5′-tgcctgcttcaccaccttct-3′ (antisense, 600 nM); human Glo1: 5′-ctctccagaaaagctacactttgag-3′ (sense, 400 nM), 5′-cgagggtctgaattgccattg-3′ (antisense, 400 nM), 5′-FAM-tgggtcgcatcatcttcagtgccc-TAMRA-3′ (TaqMan Probe, 200 nM); human β-actin: 5′-cactcttccagccttccttcc-3′ (sense, 600 nM), 5′-acagcactgtgttggcgtac-3′ (antisense, 600 nM), 50-TEXASRED-tgcggatgtccacgtcacacttca-BHQ-3′ (TaqMan Probe, 200 nM). PCR reactions were performed in a total volume of 25 μl, containing 250 ng of cDNA, 1X Brilliant (or 1x Brilliant SYBR GREEN) QPCR master mix (Agilent Technology), 0.5 μl of ROX Reference Dye (Agilent Technology) and a concentration of specific primers and probes. The thermal cycling conditions were as follows: 1 cycle at 95 °C for 10 min, followed by 45 cycles at 95 °C for 20 s and 55–60 °C for 1 min. Data for comparative analysis of gene expression were obtained using the 2(-Delta Delta C(T)) method [50].

2.4. Antibodies

Primary antibodies used in the present study included the following: mouse anti-Methylglyoxal-AGE (Arg-Pyrimidine) mAb (clone 6B) (BioLogo, Hamburg, Germany); rabbit anti-Nrf2 pAb (Bioss Antibodies, Sial, Rome, Italy); rabbit anti-Nrf2 pAb (C-20) (Santa Cruz Biotechnology); rabbit anti-Nrf2 pAb (ab31163, Abcam); rabbit anti-Nrf2 mAb [EP1808Y] (AB62352, Abcam); rabbit anti-c-Jun pAb (H-79) (Santa Cruz Biotechnology); mouse anti-phospho-c-Jun mAb (KM-1) (Santa Cruz Biotechnology); mouse anti-Heme Oxygenase 1 mAb [HO-1-1] (Abcam); rabbit anti-Bax pAb (N20) (Santa Cruz Biotechnology); rat anti-Glyoxalase 1 mAb (6F10) (Santa Cruz Biotechnology); mouse anti-p-JNK mAb (G-7) (Santa Cruz Biotechnology); rabbit anti Caspase-3 pAb (9662, Cell Signaling Technology); rabbit anti phospho-Erk5 (Thr218/Tyr220) pAb (3371, Cell Signaling Technology); mouse anti-Bcl-2 mAb (DAKO, Milan, Italy); mouse anti-Cytochrome c (Cyt c) mAb (BD Pharmingen, Milan, Italy); mouse anti-Cyt c oxidase subunit IV (Cox IV) mAb (Molecular Probes, Monza, Italy); goat anti-mouse KLF4 pAb (AF3158, R&D Systems); goat anti-human KLF4 pAb (AF3640, R&D Systems); mouse anti-β-actin mAb (C4) (Santa Cruz Biotechnology); rabbit anti-lamin β1 pAb (H-90) (Santa Cruz Biotechnology); mouse anti-α-tubulin mAb (Sigma-Aldrich).

2.5. Protein extraction and western blotting

Extraction of total proteins was performed by lysing cells in pre-cooled radioimmunoprecipitation assay (RIPA) lysis buffer. Lysates enriched for mitochondria proteins were prepared by resuspending cells in Mitobuffer and performing subcellular fractionation as described previously [51]. For nuclear extracts, a FractionPREP Cell Fractionation kit (Biovision, Vinci-Biochem, Florence, Italy) was used. Protein concentration in cell extracts was determined spectrophotometrically using the BCA protein assay kit (Pierce, USA).

For WB, cell extract supernatants containing an equal amount of proteins (20 μg) were treated with Laemmli buffer, boiled for 5 min, resolved on either 10, 12 or 15% SDS-PAGE, and then blotted onto a nitrocellulose membrane using iBlot Dry Blotting System (Invitrogen). Unoccupied protein-binding sites were blocked by incubation with Roti-Block for 1 h at room temperature, and membranes were then incubated overnight at 4 °C with appropriate dilutions of specific primary antibodies. Subsequently, membranes were washed three times with TBS/0.1% Tween-20 (TBST) for 10 min each, and incubated for 1 h at room temperature with the appropriate horseradish peroxidase (HRP)-conjugated secondary antibody (Jackson ImmunoResearch) diluted 1:10000 in TBST. After three washes with TBST, antigen-antibody complexes were then visualized by chemiluminescent detection of peroxidase activity using the ECL system (Amersham Pharmacia, Milan, Italy). As an internal control for protein loading, all membranes were subsequently stripped in stripping buffer (100 mM 2-ME, 2% SDS, and 62.5 mM Tris-HCl, pH 6.8), and re-probed with antibodies for housekeeping proteins, including α-tubulin, β-actin and lamin β1.

Protein bands from western blots were quantified by densitometry using the ImageJ software, and their relative amounts were normalized

to the levels of housekeeping proteins serving as internal loading controls.

2.6. Immunohistochemical analysis

The study was performed according to the standards of the Institutional Ethical Committee and the Helsinki Declaration, and was approved by the ethic institutional review board for "Biobanking and use of human tissue for experimental studies" of the Pathology Services ("Azienda Ospedaliera Città della Salute e della Scienza" of Turin, and Department of Medical Sciences of the University of Turin, Italy). All patient records were anonymized and de-identified prior to analysis.

Histological samples of human CCM lesions were obtained from archived, formalin-fixed, paraffin-embedded surgically resected CCM specimens retrieved from the Department of Anatomy and Diagnostic Histopathology at the University Hospital "Città della Salute e della Scienza" of Turin, Italy. At the time of neurosurgery, an informed consent was asked by neurosurgeons to patients (or legal representatives) for scientific use of residual materials, according to Institutional Rules defined by the Ethical Committee of the University Hospital "Città della Salute e della Scienza" of Turin. Only archived specimens from KRIT1 loss-of-function mutation carriers with confirmed diagnosis of CCM by both neuroradiological and histopathological analyses were included in the study. Most of the selected CCM specimens were linked to patients carrying multiple CCM lesions.

Histological serial sections (2 μm thick) of selected paraffin-embedded CCM specimens were prepared and routinely stained with hematoxylin and eosin (H&E). Two pathologists independently reviewed the H&E-stained slides, whereas additional sections, collected on superfrost plus slides, were used for immunohistochemical analysis.

Immunohistochemical (IHC) reactions were performed with a Ventana Autostainer Benchmark Ultra (Ventana Medical Systems, Inc.) as previously described [18]. Briefly, histological sections were deparaffinized, rehydrated, and subjected to a 36-min cycle at boiling temperature in citrate buffer (pH 6.0) for antigen retrieval. Endogenous peroxidase activity was blocked by a 7-min incubation with H_2O_2 solution RPE 6%. Thereafter, the sections were incubated for 32 min at 37 °C with an anti-Nrf2 primary antibody (diluted 1:100), followed by incubation with Discovery Universal Secondary Antibody Ventana (Roche). In particular, to confirm the specificity of IHC assays, we used two distinct anti-Nrf2 antibodies validated for IHC in human tissues, including the C-20 affinity purified rabbit polyclonal antibody (sc-722, Santa Cruz Biotechnology), and the ab31163 rabbit polyclonal antibody (lot. GR252439-11, Abcam). In addition, specific IHC analyses were also performed to detect Glo1, phospho-JNK and KLF4 protein levels (see Experimental Design, Materials and Methods in [49]). ICH labeling was then developed by a 5- to 10-min incubation with 3,3′ diaminobenzidine (DAB) + H_2O_2 substrate chromogen, which results in a brown-colored precipitate at antigen site. The sections were subsequently counterstained with hematoxylin, and digitized at 40X magnification using a Hamamatsu's High-Resolution Nanozoomer S210 whole slide scanner (Hamamatsu Photonics). Immunohistochemical variables were scored by evaluating the percentage of stained nuclei at a 40× magnification in endothelial lumens.

2.7. Affinity purification and identification of MG-derived argpyrimidine protein adducts

Purification and identification of MG-derived AP protein adducts was performed according to Sakamoto et al. [43].

2.8. Enzymatic activity assays

Cell extract preparation for enzymatic activity assays was performed as previously described [42]. Briefly, cells were harvested and suspended in 10 mM phosphate buffer pH 7.0, containing 1 mM dithiothreitol (DTT) and 0.1 mM phenylmethanesulphonyl fluoride (PMSF). Cell suspensions were then homogenized with a Potter-Helvehjem homogenizer, centrifuged at 13,000 × *g* for 30 min and the resulting cell extracts used for enzymatic activities and protein content measurements.

Glo1 activity was assayed according to Mannervik et al. [52]. The assay solution contained 0.1 M sodium-phosphate buffer (PBS) pH 7.2, 2 mM MG, and 1 mM GSH. The reaction was monitored spectrophotometrically by following the increase of absorbance at 240 nm and 25 °C, attributable to the formation of S-D-lactoylglutathione. One unit activity is defined as 1 μmole of S-D-lactoylglutathione produced min^{-1}.

2.9. Assessment of cellular levels of reactive oxidative species

Assessment of cellular levels of reactive oxidative species, including levels of general reactive oxygen species (ROS) and reactive nitrogen species (RNS), was performed as a follow-up analysis of previously published studies [15–18] using the membrane permeable 2′–7′-dichlorofluorescin-diacetate (H_2DCF-DA) fluorogenic dye (Invitrogen). Following cleavage of the acetate groups by intracellular esterases, the resultant dichlorofluorescin (DCFH) is trapped intracellularly due to its hydrophilicity, and oxidized by various ROS/RNS to form the highly fluorescent 2′,7′-dichlorofluorescein (DCF), which can be detected by fluorescence spectrophotometry or microscopy, thus serving as an effective indicator of generalized cellular oxidative stress. Briefly, MEF and hBMEC cellular models described above were grown to confluence in complete medium, washed twice with PBS, incubated with H_2DCF-DA at a final concentration of 5 μM in PBS at 37 °C for 30 min, and analyzed by image-based cytometry with a Tali® Image-Based Cytometer (Invitrogen). Raw data were processed using the Flowing software (v.2.5.0, by Perttu terho, University of Turku, Finland). Fluorescence readings were expressed as either relative fluorescence units (RFU) or relative ROS/RNS level units. More specific measurements of mitochondrial $O_2^{\bullet -}$ and H_2O_2 levels in the same cellular models were performed previously using the superoxide indicator MitoSOX Red [15] and the H_2O_2 sensor pHyPer-dMito (mt-HyPer probe) [18]. In addition, further measurements of cellular H_2O_2 levels were performed with the Amplex® Red Hydrogen Peroxide/Peroxidase Assay Kit (A22188, Invitrogen) (see Experimental Design, Materials and Methods, and Fig. 1 in [49]). However, as it is still not possible to exclude the involvement of other oxidative species not yet analyzed in addition to $O_2^{\bullet -}$ and H_2O_2, we resort to the use of the generic term ROS to refer to $O_2^{\bullet -}$ and H_2O_2 as well as to secondary oxidative products that might be implicated without certainty, according to the recommendations of FRBM´s Editors [53].

2.10. DNA damage detection

DNA damage was detected by evaluating apurinic/apyrimidinic (AP or abasic) sites by the DNA Damage - AP sites - Assay Kit (Colorimetric) (ab65353, Abcam), according to the manufacturer's instructions. Indeed, the AP site is one of the prevalent lesions of oxidative DNA damage and its level is considered a good indicator of such damage. In particular, Abcam's DNA Damage – AP Sites – Assay utilizes the ARP (Aldehyde Reactive Probe) reagent that reacts specifically with an aldehyde group on the open ring form of AP sites. AP sites are then tagged with biotin residues that can be quantified using a streptavidin-enzyme (HRP) conjugate and an absorbance reader. Briefly, 500 ng of genomic DNA were labeled with ARP containing a biotin moiety, immobilized in microwells, and incubated with streptavidin-conjugated HRP. An HRP substrate was then added, and the absorbance (650 nm) was measured using a microplate absorbance reader. To translate the absorbance units into the number of AP sites, a standard curve was obtained using control DNA containing 40 AP sites per 10^5 bp, according to a previously published protocol [54].

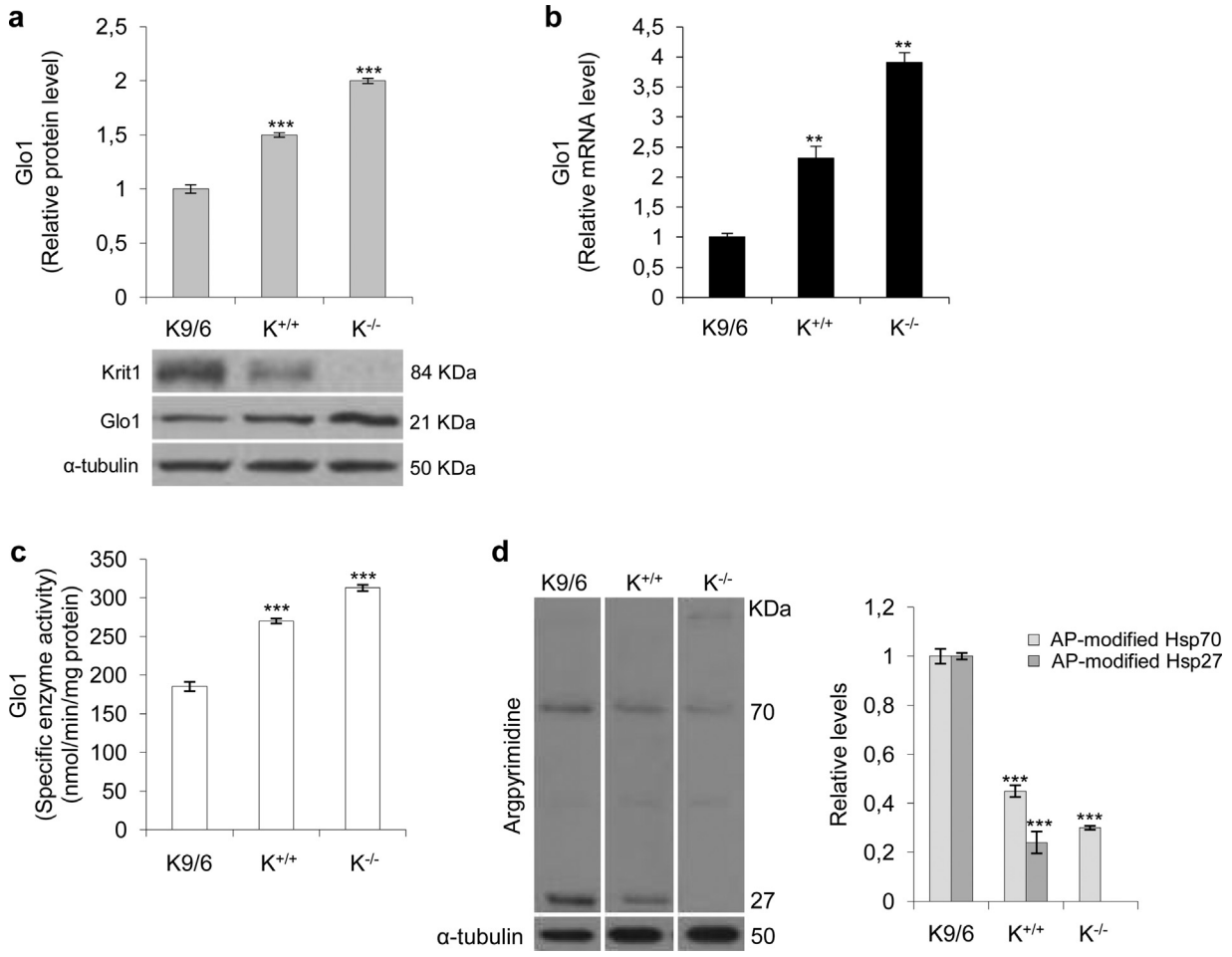

Fig. 1. KRIT1 modulates the expression of the anti-glycation enzyme Glyoxalase 1 (Glo1) and the formation of MG-derived argpyrimidine protein adducts. Wild type ($K^{+/+}$), $KRIT1^{-/-}$ ($K^{-/-}$), and $KRIT1^{-/-}$ re-expressing KRIT1 (K9/6) MEF cells grown to confluence under standard conditions were lysed and analyzed by Western blotting (**a**,**d**), qRT-PCR (**b**), and spectrophotometric enzymatic assay (**c**) as described in Materials and Methods. **a**) Representative Western blot and quantitative histogram of the relative KRIT1 and Glo1 protein expression levels. α-tubulin was used as internal loading control for WB normalization. The WB bands of Glo1 were quantified by densitometric analysis, and normalized optical density values were expressed as relative protein level units referred to average value obtained for K9/6 samples. **b)** Glo1 mRNA expression levels were analyzed in triplicate by qRT-PCR and normalized to the amount of an internal control transcript (GAPDH). Results are expressed as relative mRNA level units referred to the average value obtained for K9/6 cells, and represent the mean (± SD) of n ≥ 3 independent qRT-PCR experiments. **c)** Glo1 enzyme activity was measured in cytosolic extracts according to a spectrophotometric method monitoring the increase in absorbance at 240 nm due to the formation of S-D- lactoylglutathione. Glo1 activity is expressed in milliunits per mg of protein, where one milliunit is the amount of enzyme that catalyzes the formation of 1 nmol of S-D-lactoylglutathione per min under assay conditions. Results represent the mean (± SD) of n ≥ 3 independent experiments performed in triplicate. **d**) Representative WB and quantitative histogram of argpyrimidine (AP) adducts as detected using a specific mAb. α-tubulin was used as internal loading control for WB normalization. Western blots are representative of three separate experiments. **p ≤ 0.01 versus K9/6 cells, ***p ≤ 0.001 versus K9/6 cells. Notice that KRIT1 loss-of-function leads to a significant increase in Glo1 expression and activity, and a decrease in the intracellular levels of major AP adducts of 70 and 27 kDa.

2.11. Apoptosis detection

Apoptosis was detected by evaluating DNA fragmentation by TdT-mediated dUTP nick-end labeling (TUNEL) assay (ApoAlert® DNA Fragmentation Assay, Clontech Laboratories, Inc., Mountain View, CA, USA) [55].

2.12. Statistical analysis

Data were generated from three independent experiments and expressed as means ± standard deviation (SD). One-way analysis of variance with Dunnett's correction was used to assess differences among groups. Statistical significance, determined by Student's *t*-test, was set at $p < 0.05$.

3. Results

3.1. KRIT1 modulates the expression of the anti-glycation enzyme Glyoxalase 1 and the formation of MG-derived argpyrimidine protein adducts

Previously, we showed that KRIT1 loss-of-function is associated with increased intracellular ROS levels and enhanced cell susceptibility to ROS-mediated molecular damage and cellular dysfunctions [15,16,18].

To gain further insights into the role of KRIT1 in redox-sensitive pathways and mechanisms underlying cell defense against oxidative stress, we tested the effects of KRIT1 loss-of-function on the expression levels of Glyoxalase 1 (Glo1), a major redox-dependent cytoprotective enzyme involved in distinct cellular responses to oxidative stress, including induction of epithelial-to-mesenchymal transition (EMT) and apoptosis [37,38,42,55]. To this end, we took advantage of established cellular models of CCM disease, including KRIT1-knockout MEF cells and KRIT1-silenced human brain microvascular endothelial cells

(hBMEC), which previously allowed the identification of new molecules and mechanisms involved in KRIT1 physiopathological functions, opening novel therapeutic perspectives for CCM disease [14–16,18,22,56,57].

Compared with wild-type ($K^{+/+}$) and $KRIT1^{-/-}$ MEFs re-expressing KRIT1 (K9/6) cells, $KRIT1^{-/-}$ ($K^{-/-}$) cells displayed a significantly higher expression of Glo1 both at protein (Fig. 1a) and mRNA levels (Fig. 1b), suggesting that KRIT1 loss induces the upregulation of Glo1 expression.

To determine whether the observed increase in Glo1 transcript and protein levels was paralleled by a similar trend at the functional level, Glo1 specific enzymatic activity was examined by a spectrophotometric method. The outcomes showed that Glo1 activity was significantly higher in $K^{-/-}$ than $K^{+/+}$ and K9/6 cells (Fig. 1c), suggesting that the upregulation of Glo1 caused by KRIT1 loss is paralleled by increased levels of Glo1 enzymatic activity.

Glo1 plays a key role in limiting intracellular accumulation of MG, thereby modulating the formation and effects of MG-derived protein glycation adducts [30]. Among these, argpyrimidine (AP) has been shown to play a dual role in the regulation of important cellular processes, including opposite effects on the apoptotic process, depending on its concentration and the cell context. Specifically, high levels of AP can promote cell death [39,40], whereas physiological levels are required to drive major cell survival mechanisms [43,44]. Thus, we addressed the possibility that the KRIT1 loss-dependent increase in Glo1 expression was accompanied by a decrease in the intracellular levels of AP adducts. To this end, AP levels in protein extracts from $K^{-/-}$, $K^{+/+}$ and K9/6 cells were analyzed by WB with an antibody specifically directed against AP adducts. As a result, we detected two major bands with an approximate molecular weight of 70 and 27 kDa, whose intensity was lower in $K^{-/-}$ compared to $K^{+/+}$ and K9/6 cells (Fig. 1d), indicating that the KRIT1 loss-dependent increase in Glo1 expression and activity was indeed accompanied by a drop in the intracellular levels of AP adducts.

3.2. The upregulation of Glyoxalase 1 and the downregulation of intracellular levels of argpyrimidine adducts occur also in human brain microvascular endothelial cells upon KRIT1 knockdown

To investigate whether the upregulation of Glo1 and the downregulation of AP adducts observed in $K^{-/-}$ MEF cells could be recapitulated in a different cellular model, more strictly connected to CCM disease, we used hBMEC and performed KRIT1 knockdown according to a previously optimized siRNA-based procedure [18]. Notably, this approach previously allowed us to demonstrate that KRIT1 knockdown in hBMEC leads to a significant increase in intracellular ROS levels due to defective mitophagy [18]. In line with experimental observations in $K^{-/-}$ MEF cells, we found that Glo1 was significantly upregulated in KRIT1-silenced versus control hBMEC cells both at protein (Fig. 2a), mRNA (Fig. 2b), and specific activity (Fig. 2c) levels. Furthermore, these events were accompanied by an increase in intracellular levels of oxidative species (Fig. 2d), and a reduced formation of MG-derived AP adducts (Fig. 2e), demonstrating that the upregulation of Glo1 and the downregulation of AP adducts induced by the loss-of-function of KRIT1 can occur in different cellular models, including brain microvascular endothelial cells.

3.3. The upregulation of Glo1 and the decrease of AP levels caused by KRIT1 loss are redox-dependent

While it is well known that supra-physiological levels of MG cause mitochondrial dysfunction, ROS formation, and oxidative stress-mediated cellular injury [58,59], growing evidence indicates that Glo1 induction plays an important role in molecular mechanisms underlying cellular adaptive responses to oxidative stress [29,46]. Indeed, it has been shown that the mammalian Glo1 gene contains a functional antioxidant-response element (ARE), which serves to engage Glo1 in the major cytoprotective antioxidant system controlled by Nrf2 [29], suggesting that the stress-responsive transcriptional control of Glo1 provides a combined defense against both dicarbonyl glycation and oxidative stress. Consistently, there is evidence that either MG- or H_2O_2-induced oxidative stress leads to increased Glo1 mRNA, protein and activity [29,30].

In this light, we tested whether the observed KRIT1 loss-mediated upregulation of Glo1 and depletion of AP adducts were dependent on the increase in intracellular ROS levels previously associated with KRIT1 loss-of-function [15–18], including the increase in mitochondrial superoxide anion ($O_2^{\bullet -}$) and H_2O_2 levels detected by specific mitochondrial probes [15,18]. To this end, we treated $K^{-/-}$, $K^{+/+}$ and K9/6 MEF cells with the SOD mimetic Tiron, a mitochondria-permeable superoxide scavenger [60]. The outcomes of these experiments showed that the reduction of cellular ROS/RNS levels occurring in $K^{-/-}$ cells upon treatment with Tiron (Fig. 3a) was associated with a correspondent significant reduction of Glo1 mRNA (Fig. 3b), protein (Fig. 3c) and specific activity (Fig. 3d) levels, indicating that the upregulation of Glo1 induced by KRIT1 loss is a redox-sensitive phenomenon. In addition, as assessed by WB analysis with a specific antibody, treatment of $K^{-/-}$ cells with Tiron resulted also in an increase of AP adducts up to levels found in untreated $K^{+/+}$ cells (Fig. 3e,f), indicating that the antioxidant Tiron could rescue both the increased expression of Glo1 and the decreased levels of AP adducts caused by KRIT1 loss-of-function to near-physiological levels. These results were confirmed in KRIT1-silenced hBMEC cells treated with Tiron (see Fig. 3a-c in [49]), demonstrating that KRIT1 downregulation causes a redox-sensitive upregulation of Glo1 and depletion of AP adducts in distinct cellular models of CCM disease.

3.4. KRIT1 loss-dependent upregulation of Glo1 is part of a cell adaptive response to oxidative stress involving the master redox-sensitive transcriptional regulator Nrf2

To clarify the molecular mechanism underlying the KRIT1 loss-dependent and redox-sensitive upregulation of Glo1, we investigated the possible involvement of Nrf2, the master transcription factor that coordinately regulates cellular defenses against oxidative stress through the induction of genes coding for antioxidant and detoxification enzymes, including Glo1 [23,25,29,61,62]. To this end, nuclear and cytoplasmic extracts of $K^{-/-}$, $K^{+/+}$ and K9/6 cells were analyzed to examine the activation of Nrf2 by WB assessment of its nuclear translocation. Indeed, an increased accumulation in the nucleus is a key part of the Nrf2 activation mechanism, and the WB technique remains the most widely used method to assess this change [23,61]. The outcomes of these experiments demonstrated that the nuclear to cytoplasmic ratio of Nrf2 was significantly higher in $K^{-/-}$ than $K^{+/+}$ and K9/6 cells (Fig. 4a), suggesting that Nrf2 is activated in response to the loss-of-function of KRIT1. Furthermore, consistent with the established transcriptional control of Glo1 by Nrf2 [29], the increased nuclear translocation of Nrf2 in $K^{-/-}$ versus $K^{+/+}$ and K9/6 cells (Fig. 4a) reflected the upregulation of Glo1 mRNA and protein levels (Fig. 1a,b), suggesting that KRIT1 loss-of-function leads to a sustained upregulation of the Nrf2-Glo1 antioxidant pathway.

To test whether the observed activation of Nrf2 was a consequence of the increase in intracellular ROS levels associated with KRIT1 loss-of-function [15–18], we analyzed the effects of cell treatment with the ROS scavenger Tiron, using nuclear c-Jun and phospho-c-Jun (P-c-Jun) as controls. Indeed, we previously demonstrated that nuclear levels of the phosphorylated active form of c-Jun, a critical component of the redox-sensitive dimeric transcription factor complex AP-1 (activating protein 1), are upregulated by KRIT1 loss-of-function in a redox-dependent manner [16]. As shown in Fig. 4b, the antioxidant Tiron rescued both c-Jun and Nrf2 activation occurring in $K^{-/-}$ cells near to levels of $K^{+/+}$ and K9/6 cells, demonstrating that these activations were indeed redox-sensitive events linked to KRIT1 loss-of-function. Notably,

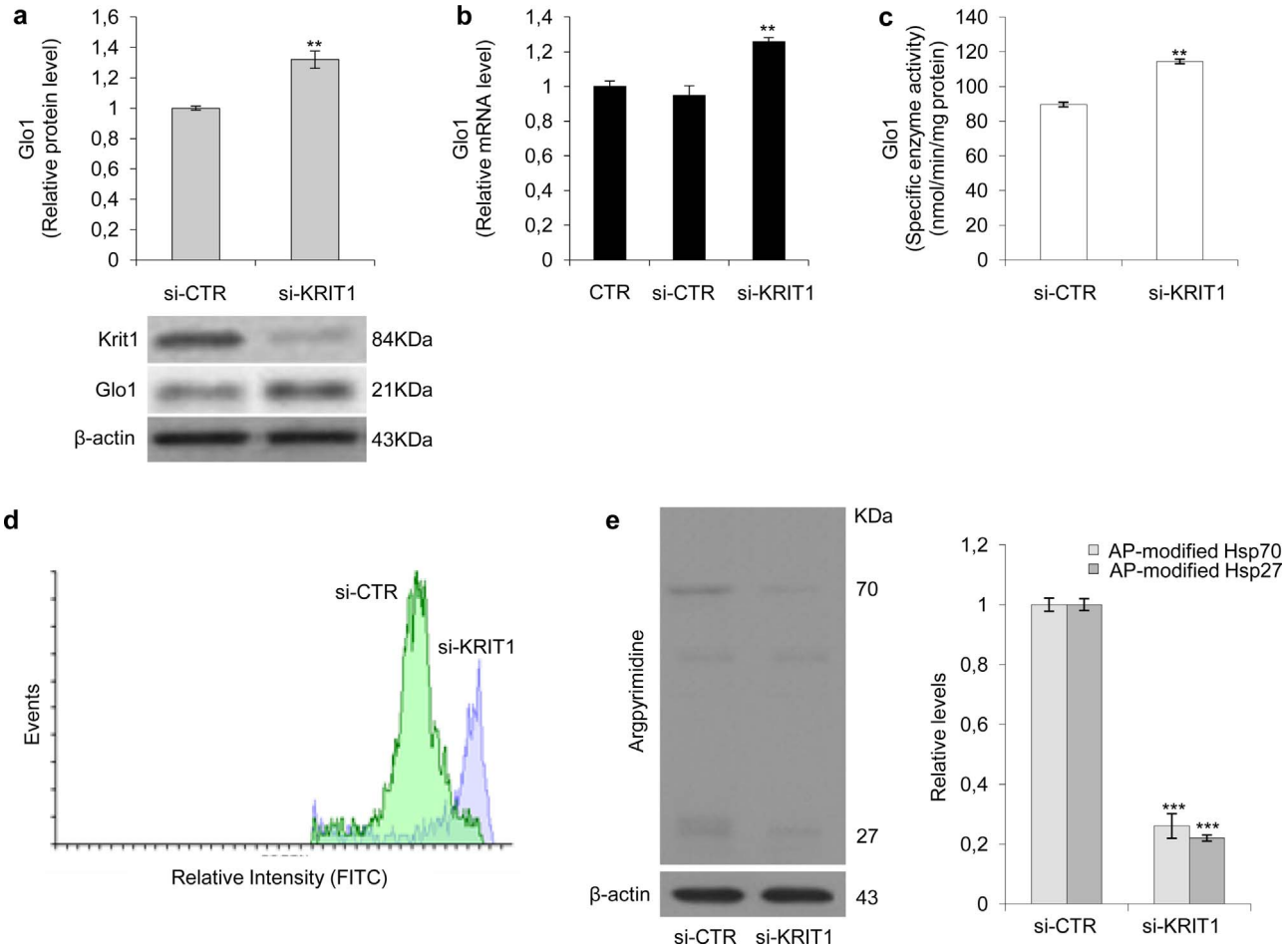

Fig. 2. The upregulation of Glyoxalase 1 (Glo1) and the downregulation of argpyrimidine adducts occur also in human brain microvascular endothelial cells upon KRIT1 knockdown. Human brain microvascular endothelial cells (hBMEC) grown under standard conditions were mock transfected (CTR) or transfected with either KRIT1-targeting siRNA (siKRIT1) or a scrambled control (siCTR). Cells were then either lysed and analyzed by Western blotting (**a,e**), qRT-PCR (**b**), and spectrophotometric enzymatic assay (**c**), or treated with H_2DCF-DA for measurement of cellular levels of general reactive oxidative species by image-based cytometry (**d**), as described in Materials and Methods. **a**) Representative WB and quantitative histogram of the relative KRIT1 and Glo1 protein expression levels in si-CTR and si-KRIT1 cells. β-actin was used as internal loading control for WB normalization. The WB bands of Glo1 were quantified by densitometric analysis, and normalized optical density values were expressed as relative protein level units referred to the average value obtained for si-CTR samples. **b)** Glo1 mRNA expression levels were analyzed in triplicate by qRT-PCR and normalized to the amount of an internal control transcript (human β-actin). Results are expressed as relative mRNA level units referred to the average value obtained for control cells (CTR), and represent the mean (± SD) of n ≥ 3 independent qRT-PCR experiments. **c)** Glo1 enzyme activity was measured in cytosolic extracts of si-CTR and si-KRIT1 cells according to a spectrophotometric method monitoring the increase in absorbance at 240 nm due to the formation of S-D-lactoylglutathione. Glo1 activity is expressed in milliunits per mg of protein, where one milliunit is the amount of enzyme that catalyzes the formation of 1 nmol of S-D-lactoylglutathione per min under assay conditions. Results represent the mean (± SD) of n ≥ 3 independent experiments performed in triplicate. **d**) Measurement of cellular levels of general reactive oxidative species. si-CTR and si-KRIT1 endothelial cells were left untreated or treated with H_2DCF-DA, and DCF fluorescence intensity was analyzed by a Tali® Image-Based Cytometer. The representative cytometer profile shows the increase in DCF fluorescence intensity in si-KRIT1 cells as compared to the control (si-CTR). **e**) Representative WB and quantitative histogram of argpyrimidine (AP) adducts in si-CTR and si-KRIT1 endothelial cells as detected using a specific mAb. β-actin was used as internal loading control for WB normalization. Western blots are representative of three separate experiments. **p ≤ 0.01 compared to control (CTR or si-CTR) cells. Notice that KRIT1 knockdown in human brain microvascular endothelial cells leads to a significant increase in Glo1 expression and activity, and a decrease in the intracellular levels of major AP adducts of 70 and 27 kDa.

the Tiron-mediated reduction of Nrf2 nuclear levels (Fig. 4b) reflected a correspondent downregulation of Glo1 (Fig. 3b,c), which is consistent with the reported redox-sensitive transcriptional regulation of Glo1 expression mediated by Nrf2 [29]. Furthermore, consistent with the activation of Nrf2, we found that the increased nuclear translocation of Nrf2 induced by KRIT1 loss-of-function (Fig. 4a,b) was associated with the upregulation of heme oxygenase-1 (HO-1) (Fig. 4c), an established Nrf2/ARE-regulated phase II antioxidant and detoxification enzyme that is primarily involved in cytoprotection against oxidative stress-induced cellular damage and apoptosis in various tissues, including the vasculature [63–65]. Specifically, WB analysis showed a marked increase in the expression levels of HO-1 in $K^{-/-}$ cells as compared with K9/6 cells (Fig. 4c), which was significantly reduced upon cell treatment with the antioxidant Tiron (Fig. 4c). All these results were recapitulated in KRIT1-silenced versus control hBMEC cells (see Fig. 4 in [49]), further supporting the finding that KRIT1 loss-of-function leads to the redox-sensitive activation of Nrf2 and consequent upregulation of its downstream targets HO-1 and Glo1.

Remarkably, as hypothesized previously [21], we could also demonstrate that even other molecular signatures already associated with KRIT1 loss-of-function, including the upregulation of ERK5 phosphorylation and KLF2/4 expression [66], are redox-dependent and can be rescued by the antioxidant Tiron both in KRIT1-knockout MEF and in KRIT1-silenced hBMEC cells (see Fig. 6 in [49]), suggesting that they could be part of the abnormal adaptive response to altered redox homeostasis and signaling identified herein.

3.5. *Defective autophagy and JNK activation contribute to the sustained upregulation of Nrf2 and Glo1*

Previously, we found that the upregulation of c-Jun induced by KRIT1 loss-of-function could be attributed at least in part to a redox-

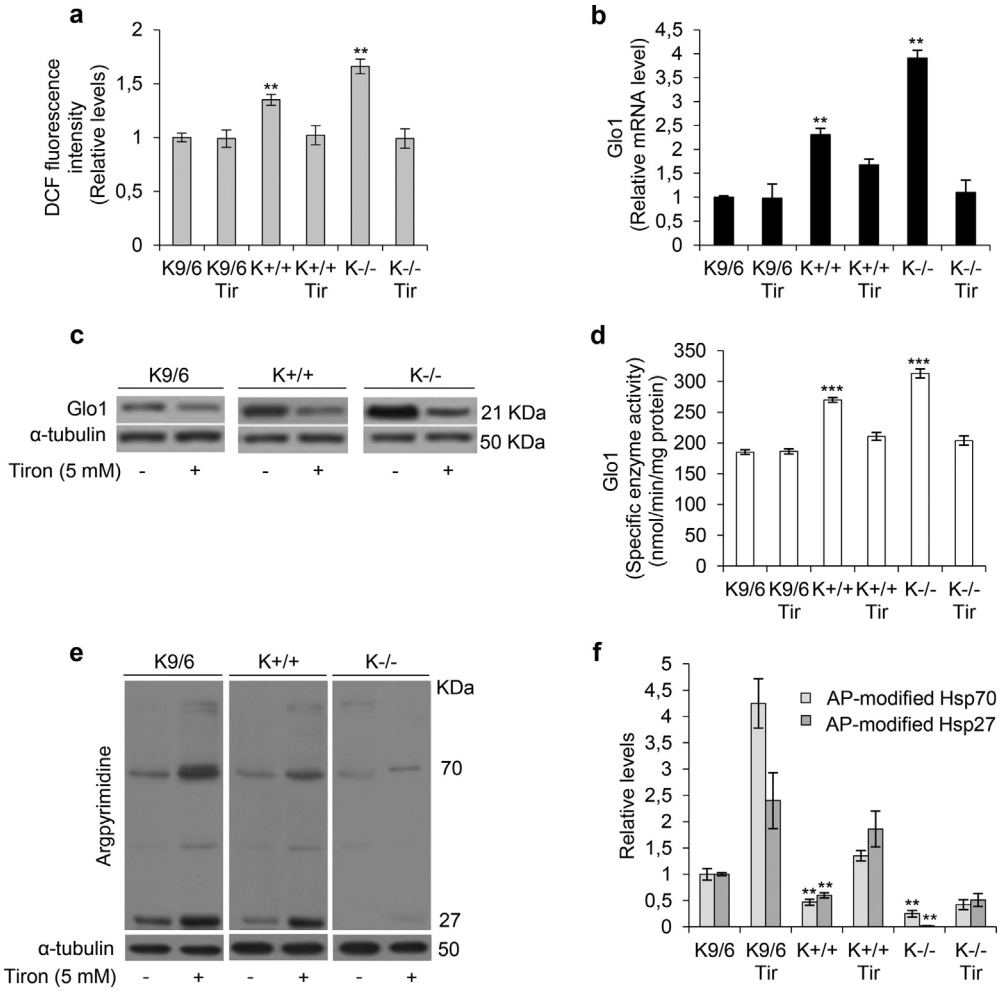

Fig. 3. The upregulation of Glyoxalase 1 (Glo1) and the decrease of argpyrimidine levels caused by KRIT1 loss are redox-dependent. Wild type ($K^{+/+}$), $KRIT1^{-/-}$ ($K^{-/-}$), and $KRIT1^{-/-}$ re-expressing KRIT1 (K9/6) MEF cells grown to confluence under standard conditions were either mock-pretreated or pretreated with the ROS scavenger Tiron (Tir). Cells were then either treated with H_2DCF-DA for measurement of cellular levels of general reactive oxidative species by image-based cytometry (**a**), or lysed and analyzed by qRT-PCR (**b**), Western blotting (**c,e**), and spectrophotometric enzymatic assay (**d**) as described in Materials and Methods. **a**) Measurement of cellular levels of general reactive oxidative species. Cells mock-pretreated or pretreated with Tiron (Tir) were left untreated or treated with H_2DCF-DA, and DCF fluorescence intensity was analyzed by a Tali® Image-Based Cytometer. Fluorescence readings were expressed as relative units of DCF fluorescence intensity referred to the average value obtained for K9/6 cells. **b-d)** Glo1 mRNA, protein and specific activity levels in cells mock-pretreated (-) or pretreated (+) with Tiron (Tir) were analyzed and expressed as described in Fig. 1a-c. **e-f)** Representative WB (**e**) and quantitative histogram (**f**) of intracellular levels of argpyrimidine (AP) adducts in cells mock-pretreated (-) or pretreated (+) with Tiron (Tir). WB analysis and densitometric quantification of WB bands were performed as described in Fig. 1d. Results are representative of n ≥ 3 independent experiments, and histograms represent quantifications expressed as means ± SD. **p ≤ 0.01 versus K9/6 cells; ***p ≤ 0.001 versus K9/6 cells. Notice that the normalization of intracellular ROS levels induced by cell pretreatment with the antioxidant Tiron was accompanied by the rescue of Glo1 upregulation to near-physiological levels, as well as by increased levels of AP adducts.

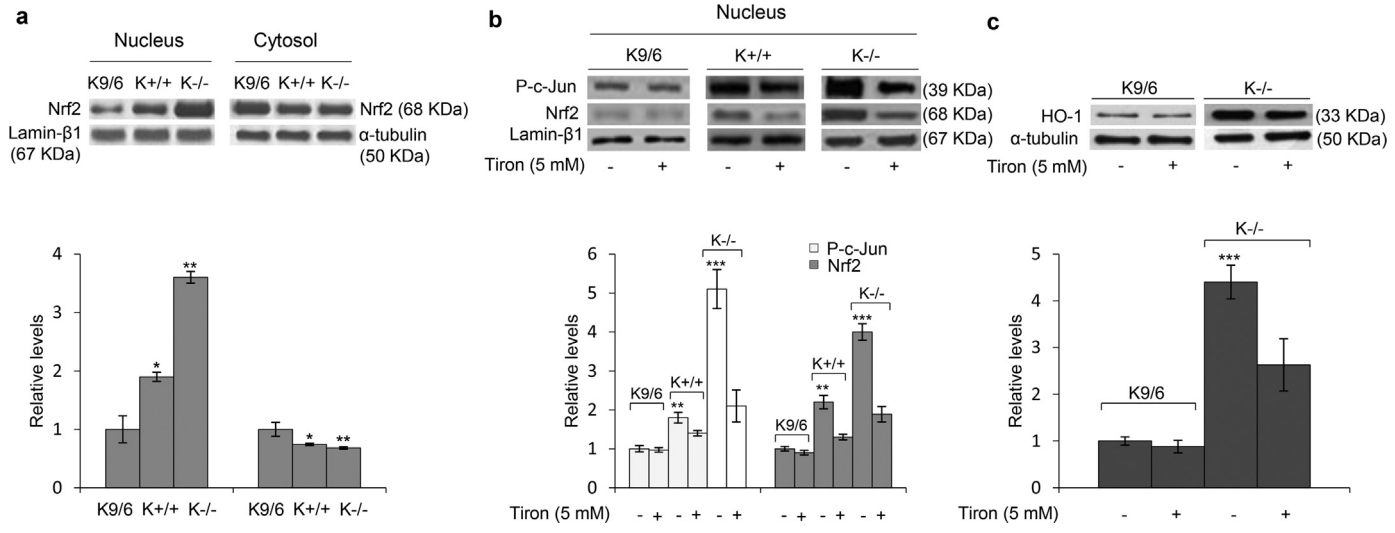

Fig. 4. KRIT1 loss-dependent upregulation of Glo1 is part of a cell adaptive response to oxidative stress involving the master redox-sensitive transcriptional regulator Nrf2. Wild type ($K^{+/+}$), $KRIT1^{-/-}$ ($K^{-/-}$), and $KRIT1^{-/-}$ re-expressing KRIT1 (K9/6) MEF cells grown to confluence under standard conditions were left untreated (**a**) or either mock-pretreated (-) or pretreated (+) with the ROS scavenger Tiron (**b**,**c**). Nuclear and cytoplasmic fractions (**a**,**b**) or total cell extracts (**c**) were then obtained and analyzed by Western blotting for the indicated proteins as described in Section 2. Nuclear levels of p-c-Jun were used as a control of redox-dependent effect of KRIT1 loss-of-function [16]. Lamin-β1 and α-tubulin were used as internal loading controls for WB normalization of nuclear and total/cytoplasmic proteins, respectively. (**a,b,c**) The histograms below their respective Western blots represent the mean (± SD) of the densitometric quantification of three independent experiments. *p < 0.05 versus K9/6 cells, **p ≤ 0.01 versus K9/6 cells, ***p ≤ 0.001 versus K9/6 cells. Notice that the upregulation of c-Jun and p-c-Jun nuclear levels induced by KRIT1 loss-of-function is paralleled by a marked nuclear accumulation of Nrf2 (**a,b**) and the upregulation of its downstream effector HO-1 (**c**), both of which are significantly reverted by cell treatment with the ROS scavenger Tiron (**b,c**).

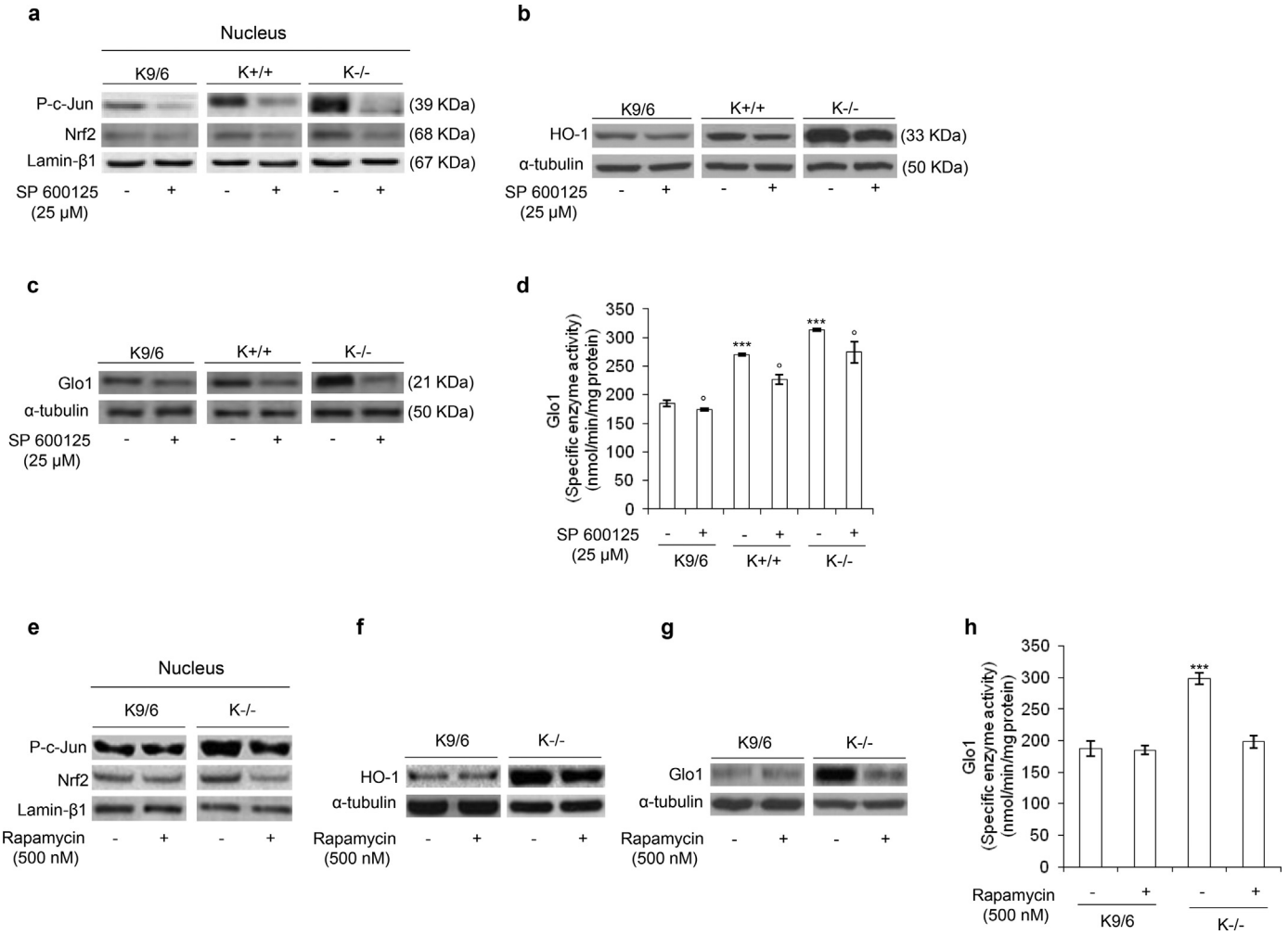

Fig. 5. Defective autophagy and JNK activation associated with KRIT1 loss-of-function contribute to the sustained upregulation of Nrf2 and its downstream effectors HO-1 and Glo1. Wild type ($K^{+/+}$), $KRIT1^{-/-}$ ($K^{-/-}$), and $KRIT1^{-/-}$ re-expressing KRIT1 (K9/6) MEF cells grown to confluence under standard conditions were either mock-pretreated (-) or pretreated (+) with the JNK inhibitor SP600125 (**a-d**), or the autophagy inducer Rapamycin (**e-h**). Nuclear and cytoplasmic fractions or total cell extracts were then obtained and analyzed by Western blotting (**a-c, e-g**) and spectrophotometric enzymatic assay (**d,h**) for the indicated proteins, as described in Materials and Methods and Fig. 1a-c. Nuclear levels of p-c-Jun were used as a control of redox-dependent effect of KRIT1 loss-of-function. Lamin-β1 and α-tubulin were used as internal loading controls for WB normalization of nuclear and total/cytoplasmic proteins, respectively. Histograms represent the mean (± SD) of n ≥ 3 independent experiments performed in triplicate. **p ≤ 0.01 and ***p ≤ 0.001 versus K9/6 cells; °p ≤ 0.05 and °°p ≤ 0.01 versus mock-pretreated (-) cells. Notice that the redox-sensitive nuclear accumulation of Nrf2 and upregulation of its downstream effectors HO-1 and Glo1 induced by KRIT1 loss-of-function were significantly reverted by cell treatment with either the JNK inhibitor SP600125 (**a-d**) or the autophagy inducer Rapamycin (**e-h**).

dependent activation of c-Jun NH_2-terminal kinase (JNK), a major upstream regulator of c-Jun [16]. Given that JNK has been reported to modulate also the activation of Nrf2 [61], we addressed the possibility that the redox-sensitive phosphorylation/activation of JNK associated with KRIT1 loss-of-function [16] could reside upstream of the upregulation of Nrf2 and its targets HO-1 and Glo1. Consistently, treatment of $K^{-/-}$ cells with the SP600125 JNK inhibitor under the same conditions previously shown to normalize phospho-c-Jun levels [16] resulted in a significant inhibition of the increased nuclear localization of Nrf2 (Fig. 5a), and accompanying upregulation of HO-1 (Fig. 5b) and Glo1 (Fig. 5c,d) observed in untreated $K^{-/-}$ cells, indicating that these effects are indeed influenced by the redox-sensitive activation of JNK.

In addition, given our previous findings demonstrating that KRIT1 loss-of-function causes defective autophagy [18], we tested whether the sustained activation of Nrf2 observed in KRIT1-null cells could be reversed by autophagy inducers, such as rapamycin. Indeed, whereas autophagy can be included in the cellular antioxidant systems as it contributes to clearing cells of damaged ROS-generating organelles and harmful oxidized biomolecules [67,68], there is clear evidence that defective autophagy results in prolonged Nrf2 activation due to accumulation of p62, a selective autophagy substrate that can bind and sequester Keap1, the negative regulator of Nrf2 [69,70]. Using the same experimental conditions previously shown to rescue molecular phenotypes associated with defective autophagy, including ROS and p62 accumulation [18], we found that treatment of $K^{-/-}$ cells with rapamycin reduced both the increased nuclear localization of phospho-c-Jun and Nrf2 (Fig. 5e), and the upregulation of HO-1 and Glo1 (Fig. 5f-h), showing that defective autophagy underlies these KRIT1 loss-dependent effects.

Taken together, these results suggest that defective autophagy and redox-dependent activation of JNK induced by KRIT1 loss-of-function contribute to the redox-sensitive activation of Nrf2 and consequent upregulation of its downstream effectors HO-1 and Glo1. In turn, the activation of these Nrf2-mediated stress response pathways could represent an adaptive mechanism by which cells sense and respond to the increased intracellular levels of oxidative species and consequent redox changes caused by KRIT1 loss-of-function.

3.6. Enhanced nuclear accumulation of Nrf2 occurs in endothelial cells lining human CCM lesions

Previously, we demonstrated that markers of either oxidative/

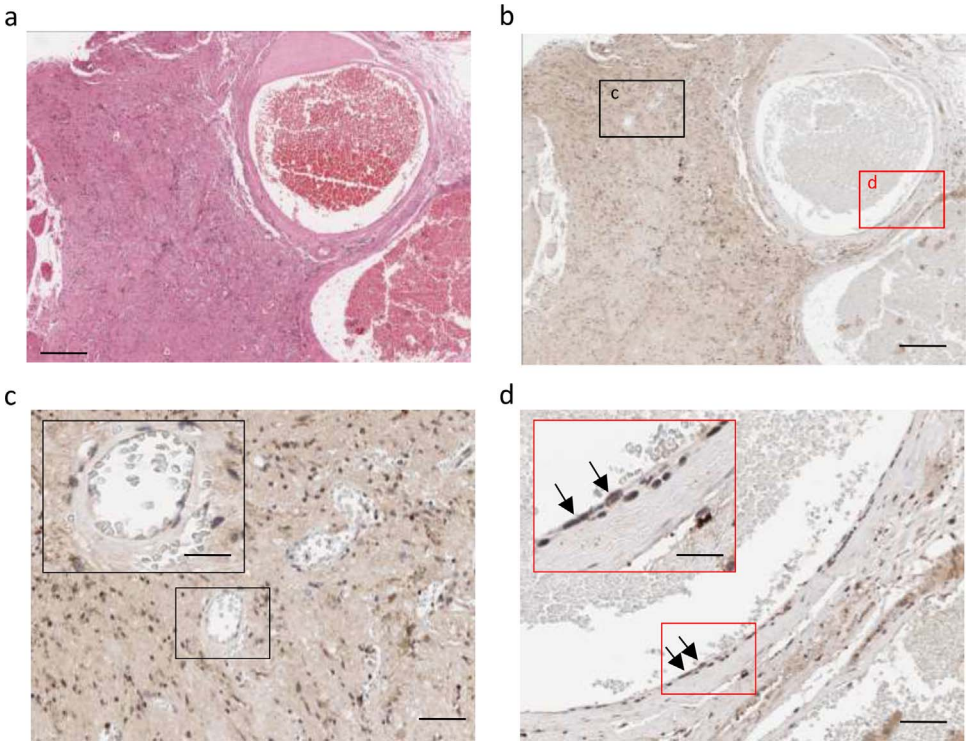

Fig. 6. Nuclear accumulation of Nrf2 in endothelial cells lining human CCM lesions. Nrf2 immunohistochemical (IHC) staining in histological sections of human CCM surgical specimens deriving from a KRIT1 loss-of-function mutation carrier. **a**,**b**) Hematoxylin/eosin (H&E) (**a**) and Nrf2 IHC (**b**) staining of a representative CCM surgical sample containing normal vessels in a perilesional area (left side, box c), which served as an internal negative control, and a large CCM lesion lined by a thin endothelium (right side and box d). **c**,**d**) Magnifications of the two representative areas indicated in panel (**b**). Notice that endothelial cells lining the lumen of normal vessels are negative for Nrf2 nuclear staining (panel **c** and magnified inset), while a significant positive Nrf2 nuclear staining is evident in endothelial cells lining the lumen of CCM lesions (black arrows, panel **d** and magnified inset). Scale bars: **a**,**b** 200 μm; **c**,**d** 50 μm, insets 30 μm.

inflammatory pathways, including P-c-Jun and COX-2, or defective autophagy, including p62, are upregulated in the endothelium of human CCM vessels [16,18]. Thereby, to examine the clinical relevance of our novel findings demonstrating the upregulation of Nrf2 in cellular models of CCM disease, we analyzed Nrf2 expression in human CCM lesions. Indeed, whereas prolonged Nrf2 activation can result from either pro-oxidant conditions [61] or defective autophagy [70], it has been reported that nuclear accumulation of Nrf2 occurs in endothelial cells of NVUs as an adaptive defense against blood-brain barrier breakdown and cerebrovascular inflammation induced by oxidative stress conditions [28,71]. Histological samples of human CCM lesions were obtained from archived paraffin-embedded surgically resected CCM specimens [18], and Nrf2 expression levels were evaluated by immunohistochemical studies using two distinct anti-Nrf2 antibodies validated for IHC in human tissues (see Materials and Methods). The IHC analysis of three distinct CCM specimens from KRIT1 loss-of-function mutation carriers with confirmed diagnosis of CCM by both neuroradiological and histopathological analyses revealed a significantly increased nuclear accumulation of Nrf2 in several endothelial cells lining the lumen of abnormally dilated CCM vessels as compared with perilesional normal vessels (Fig. 6), demonstrating that the nuclear accumulation of Nrf2 caused by KRIT1 loss-of-function occurs also *in vivo* and suggesting a potential relationship with CCM disease. Furthermore, additional IHC analyses showed that, besides enhanced nuclear localization of Nrf2, endothelial cells lining human CCM lesions express also increased levels of Glo1 and active, phosphorylated JNK (phospho-JNK) as compared with perilesional normal vessels (see Fig. 2 in [49]), thus confirming and extending the results obtained in MEF and hBMEC cellular models. Notably, the observation that activation of the JNK pathway may also occur in endothelial cells lining human CCM lesions is consistent with our previous study showing an enhanced nuclear accumulation of phospho-c-Jun in these cells [16].

Taken together, the outcomes of our IHC analyses demonstrated that only endothelial cells lining human CCM lesions, but not those of perilesional normal brain vessels, showed a significant positive staining for the target antigens assayed, including Glo1, phospho-JNK, and nuclear Nrf2, suggesting that the upregulation of these antigens in brain endothelial cells is likely influenced by a combination of genetic and environmental factors.

3.7. The redox-sensitive upregulation of Glo1 induced by KRIT1 loss-of-function is associated with the downregulation of AP-modified heat shock proteins Hsp70 and Hsp27

To understand the biological significance of the observed redox-sensitive upregulation of Glo1 and consequent downregulation of intracellular levels of AP adducts induced by KRIT1 loss-of-function, we attempted to identify the 70 kDa and 27 kDa AP-modified proteins that resulted differentially expressed in $K^{-/-}$ versus $K^{+/+}$ and K9/6 MEF cells (Fig. 1d). To this end, AP-modified proteins were purified from the lysate of K9/6 MEF cells by immunoaffinity chromatography with the anti-AP mAb. Column chromatography fractions containing the eluted 70 kDa and 27 kDa AP-modified proteins were identified by SDS-PAGE and staining with Coomassie Blue (Fig. 7a). To determine their identity, the isolated 70 kDa and 27 kDa AP-modified proteins were then digested and resolved as individual peptides by HPLC. As a result, the respective internal peptides were identified as mouse heat-shock protein 70 (Hsp70) and 27 (Hsp27) upon comparison with standard sequencing databases in the public domain (BLAST) (Fig. 7a), suggesting that KRIT1 loss-of-function leads to the downregulation of AP-modified Hsp70 and Hsp27 proteins.

3.8. The redox-sensitive decrease of AP-modified Hsp70 and Hsp27 levels induced by KRIT1 loss-of-function is associated with an increased cell susceptibility to oxidative DNA damage and apoptosis

Hsp70 and Hsp27 have been described as potent anti-apoptotic proteins, being implicated in protection against apoptosis induced by a variety of physical and chemical stresses, including heat shock and oxidative stress [72–74]. Indeed, in addition to their generally accepted role in removing or repairing denatured proteins and preventing protein aggregation, Hsp27 and Hsp70 have also been shown to interact with DNA repair enzymes and related proteins involved in cell responses to oxidative stress, thus concurring in protecting cells from

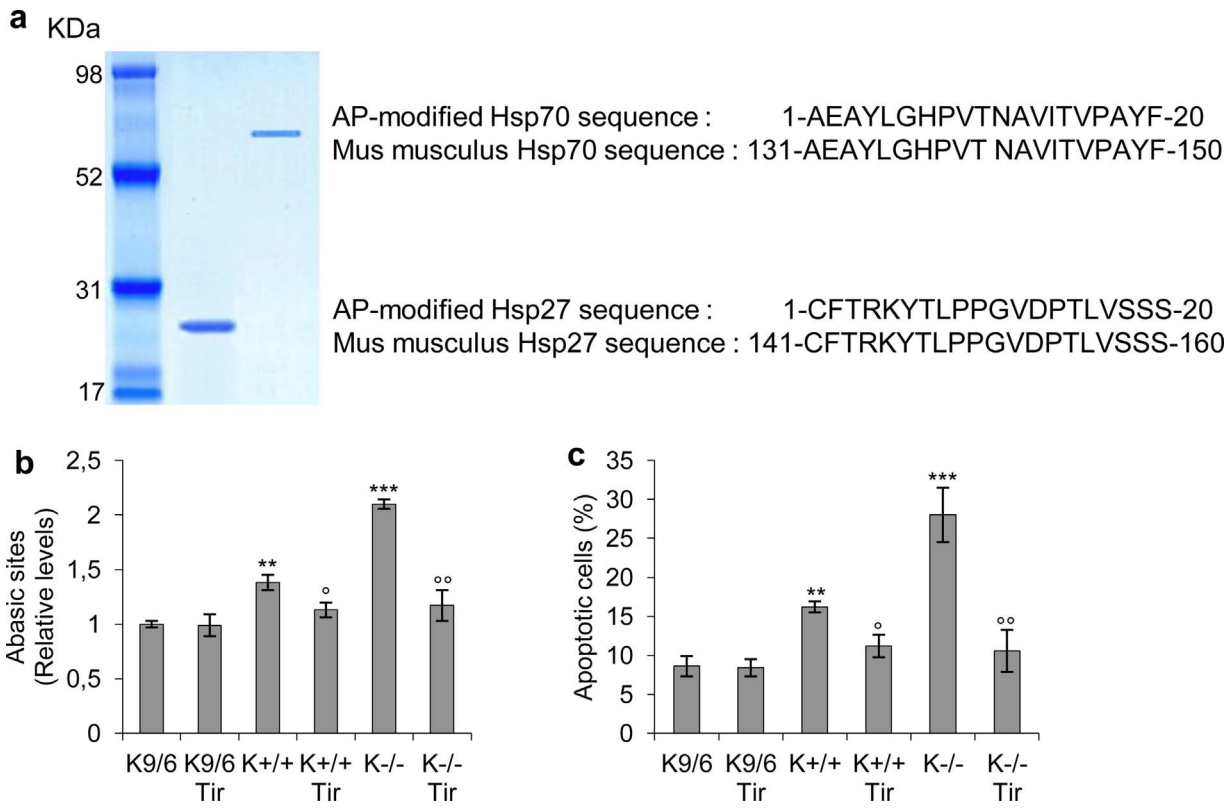

Fig. 7. KRIT1 loss-of-function is associated with a redox-sensitive downregulation of AP-modified heat shock proteins Hsp27 and Hsp70, and a redox-sensitive increase in cell susceptibility to oxidative DNA damage and apoptosis. **a)** Identification of the 70 kDa and 27 kDa AP-modified and redox-sensitive proteins downregulated in $K^{-/-}$ versus $K^{+/+}$ and K9/6 MEF cells (Figs. 1d and 3e). AP-modified proteins were purified from the lysate of K9/6 cells by immunoaffinity chromatography with an anti-AP mAb. Chromatography fractions containing the eluted 70 kDa and 27 kDa AP-modified proteins were identified by SDS-PAGE and staining with Coomassie Blue. The isolated 70 kDa and 27 kDa AP-modified proteins were then digested and resolved as individual peptides by HPLC. The respective internal peptides were identified as mouse heat-shock protein 70 (Hsp70) and 27 (Hsp27) upon comparison with standard sequencing databases in the public domain (BLAST). **b,c)** Wild type ($K^{+/+}$), KRIT1$^{-/-}$ ($K^{-/-}$), and KRIT1$^{-/-}$ re-expressing KRIT1 (K9/6) MEF cells were either mock-treated or treated with the ROS scavenger Tiron, and oxidative DNA damage (**b**) and apoptotic cell death (**c**) were evaluated by ELISA-based quantification of abasic sites in DNA and TUNEL assay, respectively. Histograms represent the mean (± SD) of n ≥ 3 independent experiments performed in triplicate. **p ≤ 0.01 and ***p ≤ 0.001 versus K9/6 cells; °p ≤ 0.05 and °°p ≤ 0.01 versus untreated cells. Notice that cell treatment with Tiron rescued the enhanced background levels of DNA abasic sites (**b**) and apoptosis (**c**) induced by KRIT1 loss-of-function ($K^{-/-}$ cells) near to levels observed in $K^{+/+}$ cells.

oxidative DNA damage [75–77]. In particular, emerging evidence demonstrates that AP modification of Hsp27 is necessary for its cytoprotective effects against oxidative damage and apoptosis [43,78,79]. In this light, our finding that KRIT1 loss-of-function is associated with a decrease in the AP-modified Hsp70 and Hsp27 levels prompted us to test whether this reduction could correlate with an enhanced cell susceptibility to oxidative DNA damage and apoptosis. Consistently, when we evaluated oxidative DNA damage and apoptotic cell death by ELISA-based quantification of abasic sites in DNA and TUNEL assay respectively, we found a significant increase in the background levels of abasic sites and apoptotic cells in $K^{-/-}$ versus $K^{+/+}$ and K9/6 MEF cells (Fig. 7b,c). Notably, cell pre-treatment with Tiron leading to the normalization of AP levels in $K^{-/-}$ cells (Fig. 3e,f) also resulted in the rescue of enhanced background levels of DNA abasic sites and apoptosis near the levels observed in $K^{+/+}$ cells (Fig. 7b,c), suggesting that the redox-sensitive decrease of AP-modified Hsp70 and Hsp27 levels induced by KRIT1 loss-of-function is positively correlated with and may contribute to increased cell susceptibility to oxidative DNA damage and apoptosis.

In addition, to address the possibility that downregulation of AP-modified Hsps and increased apoptosis susceptibility caused by KRIT1 loss-of-function were consequent to the corresponding upregulation of Glo1, we took advantage of a previously optimized siRNA-based procedure to perform Glo1 silencing and look at AP-modified Hsps and apoptosis susceptibility [55,80]. Specifically, $K^{-/-}$ and K9/6 MEF cells were transiently transfected with either a pool of four siRNAs targeting Glo1 (siGlo1) or non-targeting siRNAs used as negative control (siCtr), and AP-modified Hsp70 and Hsp27 levels and apoptosis were assayed as described in Materials and Methods. The outcomes of these experiments demonstrated that Glo1 silencing induced a significant rescue of both the downregulation of AP-modified Hsps and the increased apoptosis susceptibility associated with KRIT1 loss-of-function, suggesting a functional relationship (see Fig. 5 in [49]).

3.9. Increased susceptibility to apoptotic cell death induced by KRIT1 loss-of-function occurs through the intrinsic, mitochondria-mediated pathway

To clarify the mechanism underlying increased susceptibility to apoptotic cell death induced by KRIT1 loss-of-function and associated with a decrease in AP-modified Hsp70 and Hsp27 protein levels, we investigated the involvement of the apoptotic mitochondrial pathway by assessing the levels of key regulators, including the anti-apoptotic Bcl-2 and pro-apoptotic Bax proteins. Indeed, whereas it is well-established that the intrinsic, mitochondria-mediated pathway of cell death is especially susceptible to ROS [81], there is also clear evidence that the key regulators of this pathway are modulated by Hsps [72]. As compared with $K^{+/+}$ and K9/6 MEF cells, we found that $K^{-/-}$ cells, which are characterized by a higher apoptotic rate (Fig. 7c), presented significantly decreased levels of the anti-apoptotic Bcl-2 protein paralleled by markedly increased levels of the pro-apoptotic Bax protein (Fig. 8a). In addition, we analyzed cytochrome c (Cyt c) release into the cytosol and the activation of Caspase-3 (Casp-3), the final executioner of the apoptotic pathway [73,82]. As compared with $K^{+/+}$ and K9/6 MEF cells, a significant increase in Cyt c release into the cytosol and activation of Casp-3 was demonstrated in $K^{-/-}$ cells by WB analysis

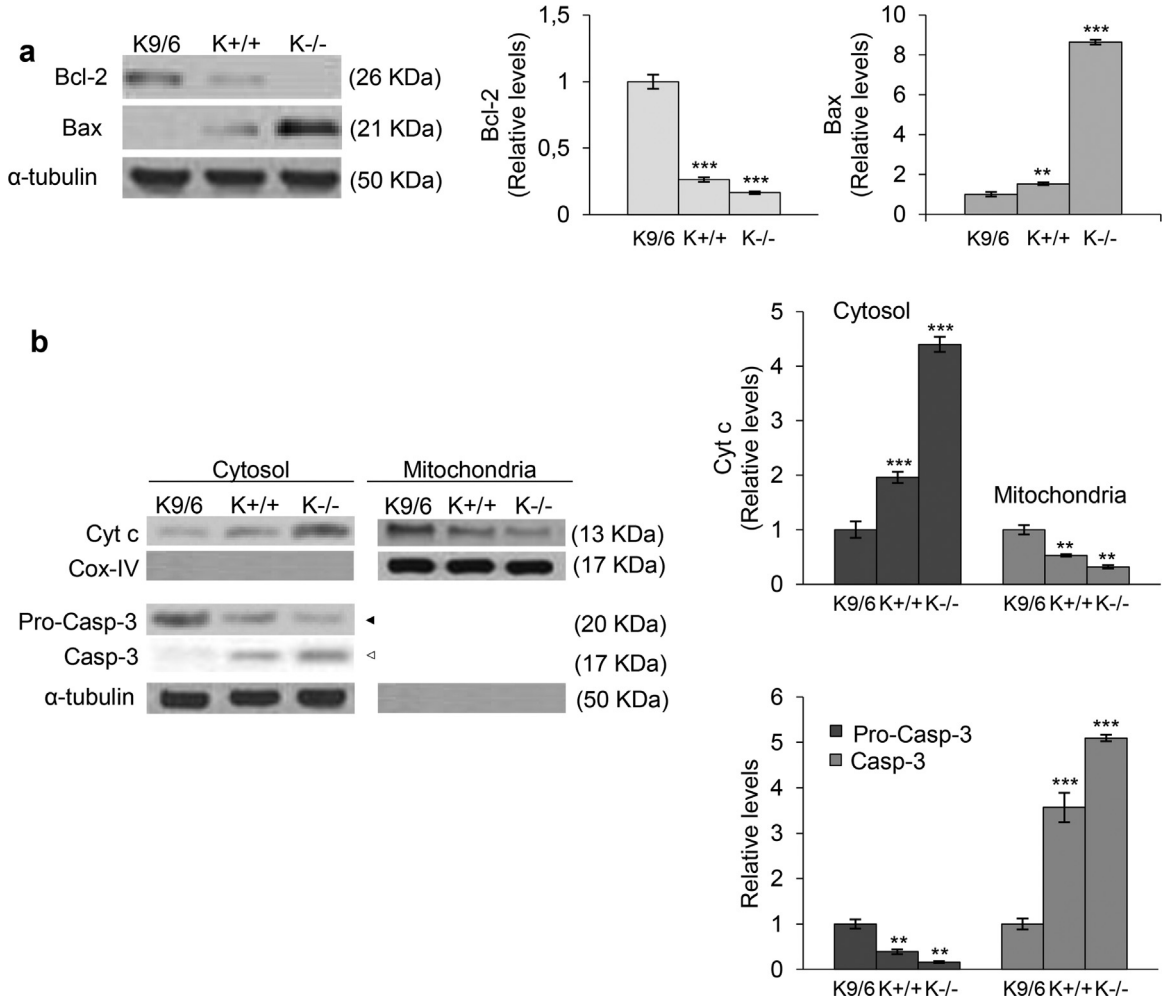

Fig. 8. The increased susceptibility to apoptotic cell death induced by KRIT1 loss-of-function occurs through the intrinsic, mitochondria-mediated pathway. Wild type ($K^{+/+}$), KRIT1$^{-/-}$ ($K^{-/-}$), and KRIT1$^{-/-}$ re-expressing KRIT1 (K9/6) MEF cells were grown to confluence under standard conditions. Total cell extracts (**a**) or mitochondria and cytosolic fractions (**b**) were then obtained, and proteins involved in the intrinsic, mitochondria-dependent apoptotic pathway, including the anti-apoptotic Bcl-2 and pro-apoptotic Bax proteins (**a**), and Cytochrome c (Cyt c) and Caspase-3 (Casp-3) (**b**), were analyzed by Western blotting as described in Materials and Methods. Cox IV and α-tubulin were used as internal loading controls for WB normalization of mitochondria and total/cytoplasmic proteins, respectively. Pro-Casp-3, intact protein; Casp-3, active fragment. A representative immunoblot is shown for each experiment. Histograms alongside their respective Western blots represent the mean (± SD) of the densitometric quantification of three independent experiments. **p ≤ 0.01 and ***p ≤ 0.001 versus K9/6 cells. Notice that the basal levels of Bcl-2 and Bax proteins in $K^{-/-}$ cells were significantly down-regulated and up-regulated, respectively, as compared with $K^{+/+}$ and K9/6 cells (**a**). In addition, a significant increase in Cyt c release into the cytosol and activation of Casp-3 was also evident in $K^{-/-}$ cells (**b**).

(Fig. 8b), suggesting that the increased susceptibility to apoptotic cell death induced by KRIT1 loss-of-function occurs through an enhanced activation of the intrinsic, mitochondria-mediated apoptotic pathway.

4. Discussion

Loss-of-function mutations of the KRIT1 gene (*CCM1*) have been clearly associated with the pathogenesis of Cerebral Cavernous Malformations (CCM) [5]. However, accumulated evidence in endothelial-specific conditional knockout mouse models demonstrates that the development of CCM lesions occurs in stochastic, spatially and temporally restricted patterns despite the pan-endothelial deletion of CCM genes [83,84], indicating that homozygous loss of *KRIT1* is not fully sufficient for CCM disease pathogenesis, and suggesting a contribution of additional factors other than disease-predisposing *KRIT1* mutations [4,12].

Our previous findings demonstrated that KRIT1 is a new important player in redox biology, showing that its loss-of-function causes the upregulation of pro-oxidant and pro-inflammatory pathways, including the redox-sensitive JNK/c-Jun/COX-2 signaling axis, and defective autophagy, resulting in perturbation of redox homeostasis and consequent molecular and cellular dysfunctions [15,16,18–20]. While pointing to a novel mechanism for CCM disease pathogenesis whereby the redox functions of KRIT1 may be relevant in preventing vascular anomalies triggered by focal oxidative stress and inflammatory events [21], these results raised new research challenges as to whether KRIT1 dysfunction exerts pleiotropic effects on multiple redox-sensitive signaling pathways and mechanisms.

Here, we extend our previous findings showing that KRIT1 loss-of-function leads to the persistent upregulation of critical cytoprotective proteins that govern cell adaptive responses to oxidative stress, including the master redox-sensitive transcription factor Nrf2 and the anti-glycation enzyme Glo1, a transcriptional target of Nrf2 that plays a critical role in the enzymatic defense against MG-mediated glycative and oxidative stress [29,46]. Furthermore, we found that the KRIT1 loss-dependent induction of these two key elements in cell survival responses to environmental stresses leads to distinct effects, including the upregulation of phase II antioxidant enzyme heme oxygenase-1 (HO-1), and the downregulation of MG-derived protein glycation adducts, such as argpyrimidine (AP) adducts. More specifically, we demonstrated that KRIT1 loss-of-function causes a drop of intracellular levels of cytoprotective AP-modified Hsp70 and Hsp27 heat shock

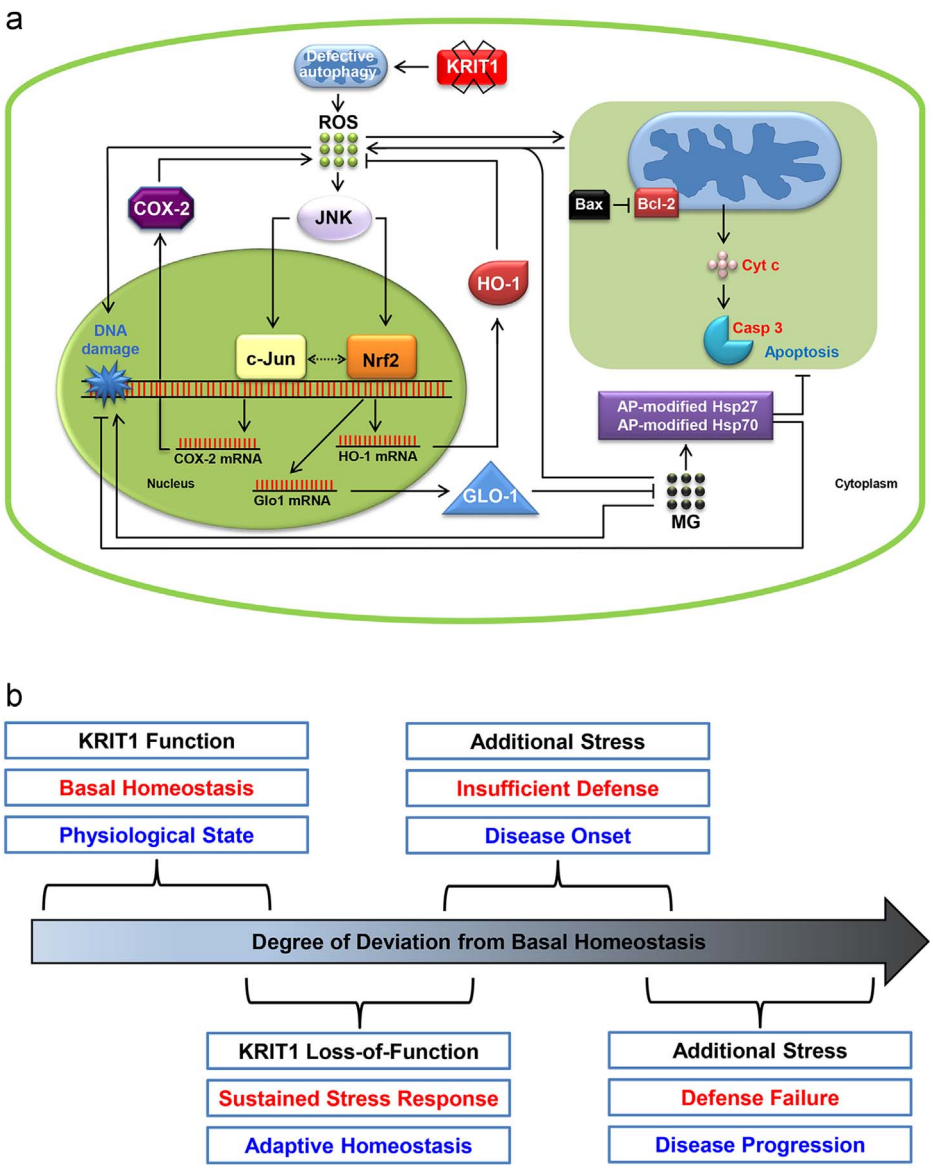

Fig. 9. Schematic models representing adaptive redox responses and cellular states associated with KRIT1 loss-of-function. **a)** Redox-sensitive pathways modulated by KRIT1 functions. KRIT1 loss-of-function causes a persistent activation of the major redox-sensitive transcription factors c-Jun and Nrf2 and consequent upregulation of downstream targets, including cycloxygenase-2 (COX-2), heme oxygenase-1 (HO-1) and glyoxalase 1 (GLO1). While the c-Jun/COX-2 axis promotes pro-oxidant and pro-inflammatory effects, the Nrf2/HO-1 and Nrf2/GLO1 pathways mediate adaptive antioxidant responses that counteract these effects by limiting ROS and MG intracellular accumulation, thus contributing to reduce a vicious cycle of oxidative stress and providing an adaptive defense for long-term cell survival. However, this sustained adaptive redox homeostasis occurs at the expense of other cytoprotective mechanisms, including the MG-dependent formation of cytoprotective AP-Hsp27 protein adducts, leading to enhanced cell susceptibility to oxidative DNA damage and apoptosis, and sensitizing cells to additional stressful insults. **b)** Spectrum of cellular states associated with KRIT1 loss-of-function. Cellular stress and defense responses associated with KRIT1 dysfunctions can be viewed as distinct but overlapping components of a spectrum of cellular states that ranges from basal homeostatic state, to adaptive stress response, insufficient defense, and defense failure, each of which can be defined in terms of the maintenance of molecular and cellular functions within an acceptable dynamic range. In turn, differences in expression and functional levels of stress-responsive proteins and adaptive defense mechanisms acting within the range of each cellular state may be influenced by genetic variation, resulting in inter-individual differences in adaptive stress responses and susceptibility to disease onset and progression. See text for details.

proteins, leading to increased levels of oxidative DNA damage and enhanced activation of the intrinsic, mitochondria-mediated apoptotic pathway. Notably, all these effects were shown to be redox sensitive, as they could be significantly reversed by cell treatment with the SOD mimetic Tiron, a mitochondria-permeable antioxidant [60], suggesting that they are part of a cell adaptive response to cope with increased intracellular ROS levels and altered redox homeostasis caused by KRIT1 loss-of-function (Fig. 9a). Accordingly, it is well established that increased ROS levels may induce oxidative damage but also activate antioxidant response mechanisms that attenuate it [62]. However, while acute, transient upregulation of the antioxidant response may eliminate the stressor and restore cellular homeostasis, chronic antioxidant responses require specific cellular adaptations and may occur at the expense of normal intracellular redox signaling, thereby affecting other redox-sensitive molecules and mechanisms, whose dysregulation may ultimately result in enhanced cell susceptibility to exogenous oxidative insults. Consistent with this paradoxical effect, there is growing evidence that persistent hyperactivation of key transcription factors involved in the maintenance of cellular redox homeostasis and defense against oxidative stress, including Nrf2 and members of the Krüppel-like factor (KLF) family, can result in an abnormal cellular stress response that paradoxically reduces oxidative stress resistance leading to disease [21,85,86]. Indeed, whereas it has been suggested that enhanced nuclear localization and activation of Nrf2 may sensitize endothelial cells to oxidative stress through a KLF2-mediated downregulation of SOD2 expression [87], the abnormally sustained activation of Nrf2 has been clearly associated with many pathogenic mechanisms of multiple human diseases, including vascular diseases [62,88,89].

In this light, our novel findings that a significant nuclear accumulation of Nrf2 occurs in both cellular models of CCM disease and endothelial cells lining the lumen of human CCM vessels suggest that the abnormally sustained activation of Nrf2 caused by KRIT1 loss-of-function may have a significant impact on CCM disease onset and progression, likely representing an either insufficient or aberrant cellular adaptive response to cope with a focal increase in oxidative challenges induced by local stressful events affecting the NVU. Further investigation in animal models of CCM disease should exploit this intriguing novel perspective toward a more comprehensive understanding of CCM disease pathogenesis and the identification of new disease biomarkers and therapeutic strategies.

Consistent with our findings, there is evidence that ROS production and stress sensitivity are significantly enhanced under conditions of Nrf2 constitutive activation [90]. Furthermore, whereas it is well-

established that Nrf2 activation exerts a major protective role against oxidative and inflammatory stress in vascular cells [25,26,64], recent emerging evidence has revealed the "dark" side of Nrf2, suggesting that its activity does not always lead to a positive outcome and may accelerate the pathogenesis of some vascular diseases [91]. Accordingly, many Nrf2 inducers exhibit hormetic properties with antioxidant beneficial effects reported at nanomolar concentrations but pro-oxidant toxic effects at higher concentrations [28,92], whereas constitutive Nrf2 activation in mice can even lead to postnatal lethality [93].

Taken together, these considerations suggest that Nrf2 may serve as a double-edged sword in cell responses to oxidative stress, with transient induction providing a feedback defense against excessive ROS generation, and sustained activation promoting abnormal adaptive modifications that affect ROS-based signal transduction, while limiting ROS accumulation and meeting requirements for cell survival under prolonged mild oxidative stress conditions [94].

With regard to potential regulatory mechanisms that could link KRIT1 loss-of-function to the Nrf2 stress response system, we found that the redox-sensitive activation of JNK may play a role, since inhibition of JNK resulted in at least partial reversion of both Nrf2 activation and accompanying upregulation of its downstream targets HO-1 and Glo1 associated with KRIT1 loss-of-function. Consistently, there is evidence that the JNK signaling pathway plays an important role in Nrf2-dependent regulation of ARE-mediated gene expression [61,95]. Furthermore, we found that the sustained activation of Nrf2 and concomitant upregulation of downstream targets observed in KRIT1-null cells can be reversed also by experimental conditions previously shown to rescue defective autophagy and p62 accumulation caused by KRIT1 loss-of-function [18], suggesting that KRIT1 dysfunctions may play an important role in the reported link between defective autophagy and sustained activation of Nrf2. Indeed, overactivation of Nrf2 can occur also as a consequence of defective autophagy through a noncanonical mechanism involving direct interaction between p62, which accumulates when the autophagic flux is impaired, and the Nrf2 negative regulator Keap1 [67,69,70,85,96].

Interestingly, besides reducing Nrf2 activation, JNK inhibition and autophagy induction reduced also c-Jun activation, suggesting that defective autophagy and redox-sensitive JNK activation previously associated with KRIT1 loss-of-function [16,18] contribute to upregulation of both c-Jun and Nrf2 redox-sensitive pathways (Fig. 9a).

Among the downstream targets of Nrf2, HO-1, also referred to as Hsp32, has been clearly implicated in cellular defenses against oxidative stress [25,97]. Indeed, the Nrf2-mediated upregulation of this antioxidant enzyme is one of the earlier events in the adaptive response to stress, and it has been proposed to play a key role in preserving vascular homeostasis during stressful conditions, including protection of the cerebral vasculature and BBB against oxidative stress-induced damage [25,27,98]. Nonetheless, whereas there is evidence that HO-1 cytoprotective activity may be impaired by inappropriate PTM occurring during cellular adaptation to chronic stress conditions, it has also been reported that the upregulation of HO-1 is not always beneficial for cells [28,99,100]. Taken together, these considerations support the possibility that the redox-sensitive upregulation of HO-1 induced by KRIT1 loss-of-function contributes to Nrf2-mediated adaptive defense mechanisms that limit a vicious cycle of ROS production and oxidative stress. However, the chronic activation of this adaptive stress response mechanism could cause HO-1 activity to be ineffective or insufficient for cytoprotective responses to additional stressful events occurring over time, leading to homeostasis imbalance and cellular dysfunction that may become irreversible (Fig. 9a,b).

Glo1, the ubiquitous key enzyme in the detoxification of α-oxoaldehydes, including MG, is emerging as another major downstream target by which Nrf2 exerts its cytoprotective stress response functions [29]. Indeed, transcriptional control of Glo1 by Nrf2 provides a stress-responsive defense against MG-mediated glycative and oxidative stress, which has been implicated in the pathophysiology of various cellular dysfunctions and diseases, including brain microvascular endothelial barrier dysfunction and vascular diseases [46–48]. Specifically, there is clear evidence that MG accumulation at supra-physiological levels causes chemical modifications of proteins, nucleic acids and lipids [31], and intensifies the mitochondrial production of ROS [58,101], ultimately exposing cells to glycative and oxidative stress and consequent pleiotropic effects, including cellular dysfunctions, DNA damage and apoptosis [42,58,59]. Nevertheless, there is also clear evidence that physiological concentrations of MG play a role in cell signaling [102], and are required to selectively modify and activate some apoptosis-protective proteins, including formation of activating argpyrimidine adducts with the anti-apoptotic heat shock protein Hsp27 [43,44], thereby playing an important role in cell homeostasis and survival. Thus, as many other molecules involved in redox signaling and cell responses to oxidative stress, both Glo1 and MG can influence biochemical pathways in both positive and negative ways, and it is known that their dose-response curve, in terms of positive and negative effects, is U-shaped. Specifically, too little Glo1 activity leads to excessive accumulation of MG and consequent enhanced glycative and oxidative stress [31,103]. By contrast, too much Glo1 activity may reduce MG levels below a physiological threshold required for PTM and activation of important signaling and cytoprotective proteins, thus paradoxically shifting the homeostatic balance toward enhanced sensitivity to environmental stresses [44,102].

In this light, our findings that KRIT1 loss-dependent upregulation of Glo1 is accompanied by a drop of AP-modified Hsp70 and Hsp27 protein levels and an enhanced cell susceptibility to oxidative damage and apoptosis, are consistent with both positive and negative effects of a sustained activation of the Nrf2-Glo1 stress-responsive pathway, as a critical adaptive mechanism to cope with persistent oxidative stress conditions [29]. Indeed, while sustained activation of the Nrf2-Glo1 stress-responsive system can contribute to reduce a vicious cycle of intracellular ROS production and oxidative stress induced by KRIT1 loss-of-function [16], providing an adaptive defense for long term cell survival, this may occur at the expense of the emerging important role of physiological levels of MG and MG-dependent protein adducts [43,44,102]. In particular, whereas the putative enhanced anti-apoptotic activity of AP-modified Hsp70 remains to be defined, there is clear evidence that AP-modified Hsp27 is endowed with enhanced cytoprotective properties, including the capacity to increase cellular resistance against a wide variety of physiological and environmental insults by limiting oxidative damage and apoptosis and facilitating cellular recovery [43,44,78,79]. Thus, the excessive downregulation of AP-Hsp27 adducts in response to an abnormal upregulation of Glo1 could result in enhanced cell susceptibility to stressful conditions. Consistently, there is evidence that Glo1 overexpression and associated reduction of physiological MG levels may increase the severity of certain brain diseases in mice [104]. In addition, the finding that increased susceptibility to apoptotic cell death induced by KRIT1 loss-of-function involves the intrinsic, mitochondria-mediated pathway is consistent with our previous results showing enhanced mitochondrial dysfunctions in distinct cellular models of CCM diseases [15,18], as well as with evidence that the intrinsic apoptotic pathway is especially susceptible to ROS [81].

5. Conclusions

The novel findings reported herein add further complexity to the already complex molecular puzzle involving KRIT1 and its pleiotropic dysfunctional effects, demonstrating that KRIT1 loss-of-function leads to an abnormal sustained activation of the Nrf2 stress defense system, including a persistent upregulation of its downstream effectors HO-1 and Glo1. Consistently, there is evidence that Nrf2 activation may lead to the simultaneous induction of HO-1 and Glo1 expression, providing a coordinated adaptive endogenous defense against both oxidative and glycative stress [105,106]. However, the sustained upregulation of these pathways due to constitutive pro-oxidant and pro-inflammatory

conditions, such as those caused by KRIT1 loss-of-function, may result in a chronic adaptive redox homeostasis that sensitizes cells to additional stressful events (Fig. 9b). Specifically, because of the incapacity of the stress-responsive defense systems to fully compensate for the absence of KRIT1 and reconstitute the basal cellular homeostasis, KRIT1 loss-of-function leads to a persistent shift from a normal homeostatic state to an adaptive stress response state, which results in cellular adaptation to a chronic mild stress condition. In the absence of additional stressful events, cytoprotective molecular adaptations allow cells to tolerate the low degree of deviation from the basal homeostatic state and achieve biological stability within a new dynamic range, thus leading to an adaptive homeostasis that preserves cell viability and function [107,108]. However, adaptive homeostasis has some physiological costs, including the cost of molecular changes required for cellular adaptation, which make cells much more vulnerable to additional internal perturbations and external insults. In fact, secondary stressful events may exceed the insufficient capacity of a chronically activated stress response system to defend the adaptive homeostatic state, leading to progressive molecular and cellular dysfunctions and disease development. Furthermore, differences in expression and functional levels of stress-responsive proteins and adaptive defense mechanisms acting within the range of either basal or adaptive homeostasis may be influenced by genetic variation, resulting in inter-individual differences in adaptive stress responses and susceptibility to disease onset and progression (Fig. 9b).

Overall, our findings extend the pleiotropic redox-sensitive functions of KRIT1 and shed new light on molecular mechanisms underlying the enhanced cell vulnerability to oxidative stress caused by KRIT1 loss-of-function, thus providing novel insights into CCM pathogenesis and treatment. Indeed, the development of pharmacological approaches aimed at helping or supplementing the cellular stress-responsive defense systems to better compensate for KRIT1 loss-of-function and restore cellular homeostasis back to the basal state, could evolve as a novel promising preventive and therapeutic option for CCM disease.

Acknowledgments

The authors wish to gratefully acknowledge Roberta Frosini, Francesca Veneziano, Irene Schiavo, Valerio Benedetti, Sara Sarri, Federica Quesada and Claudia Fornelli for providing help in some experiments. Moreover, they acknowledge the Italian Research Network for Cerebral Cavernous Malformation (CCM Italia, http://www.ccmitalia.unito.it), the Associazione Italiana Angiomi Cavernosi (AIAC, http://www.ccmitalia.unito.it/aiac) for fundamental collaboration and support, and Raffaella Mastrocola, Francesca Retta and Santina Barbaro for helpful discussion.

This work was supported by the Telethon Foundation (grant GGP15219 to SFR), the University of Torino (local research grants 2012–2016 to SFR), and the University of Perugia (local research grants 2014 to CA).

References

[1] S. Batra, D. Lin, P.F. Recinos, J. Zhang, D. Rigamonti, Cavernous malformations: natural history, diagnosis and treatment, Nat. Rev. Neurol. 5 (2009) 659–670.
[2] D. Rigamonti, Cavernous Malformations of the Nervous System, Cambridge University Press, 2011.
[3] M. Fontanella, Cerebral Cavernous Malformations, Minerva Medica ISBN:13 978-88-7711842-4, 2015.
[4] E. Trapani, S.F. Retta, Cerebral cavernous malformation (CCM) disease: from monogenic forms to genetic susceptibility factors, J. Neurosurg. Sci. 59 (2015) 201–209.
[5] H. Choquet, L. Pawlikowska, M.T. Lawton, H. Kim, Genetics of cerebral cavernous malformations: current status and future prospects, J. Neurosurg. Sci. 59 (2015) 211–220.
[6] A. Glading, J. Han, R.A. Stockton, M.H. Ginsberg, KRIT-1/CCM1 is a Rap1 effector that regulates endothelial cell-cell junctions, J. Cell Biol. 179 (2007) 247–254.
[7] W.Z. Liu, K.M. Draheim, R. Zhang, D.A. Calderwood, T.J. Boggon, Mechanism for KRIT1 release of ICAP1-mediated suppression of integrin activation, Mol. Cell 49 (2013) 719–729.
[8] J. Zhang, R.E. Clatterbuck, D. Rigamonti, D.D. Chang, H.C. Dietz, Interaction between krit1 and icap1alpha infers perturbation of integrin beta1-mediated angiogenesis in the pathogenesis of cerebral cavernous malformation, Hum. Mol. Genet. (2001).
[9] R.A. Stockton, R. Shenkar, I.A. Awad, M.H. Ginsberg, Cerebral cavernous malformations proteins inhibit Rho kinase to stabilize vascular integrity, J. Exp. Med. 207 (2010) 881–896.
[10] K.J. Whitehead, A.C. Chan, S. Navankasattusas, W. Koh, N.R. London, J. Ling, A.H. Mayo, S.G. Drakos, C.A. Jones, W. Zhu, D.A. Marchuk, G.E. Davis, D.Y. Li, The cerebral cavernous malformation signaling pathway promotes vascular integrity via Rho GTPases, Nat. Med. 15 (2009) 177–184.
[11] L. Maddaluno, N. Rudini, R. Cuttano, L. Bravi, C. Giampietro, M. Corada, L. Ferrarini, F. Orsenigo, E. Papa, G. Boulday, E. Tournier-Lasserve, F. Chapon, C. Richichi, S.F. Retta, M.G. Lampugnani, E. Dejana, EndMT contributes to the onset and progression of cerebral cavernous malformations, Nature 498 (2013) 492–496.
[12] H. Choquet, E. Trapani, L. Goitre, L. Trabalzini, A. Akers, M. Fontanella, B.L. Hart, L.A. Morrison, L. Pawlikowska, H. Kim, S.F. Retta, Cytochrome P450 and matrix metalloproteinase genetic modifiers of disease severity in Cerebral Cavernous Malformation type 1, Free Radic. Biol. Med. 92 (2016) 100–109.
[13] M. Corr, I. Lerman, J.M. Keubel, L. Ronacher, R. Misra, F. Lund, I.H. Sarelius, A.J. Glading, Decreased Krev interaction-trapped 1 expression leads to increased vascular permeability and modifies inflammatory responses in vivo, Arterioscler. Thromb. Vasc. Biol. 32 (2012) 2702–2710.
[14] C.C. Gibson, W. Zhu, C.T. Davis, J.A. Bowman-Kirigin, A.C. Chan, J. Ling, A.E. Walker, L. Goitre, S. Delle Monache, S.F. Retta, Y.T. Shiu, A.H. Grossmann, K.R. Thomas, A.J. Donato, L.A. Lesniewski, K.J. Whitehead, D.Y. Li, Strategy for identifying repurposed drugs for the treatment of cerebral cavernous malformation, Circulation 131 (2015) 289–299.
[15] L. Goitre, F. Balzac, S. Degani, P. Degan, S. Marchi, P. Pinton, S.F. Retta, KRIT1 regulates the homeostasis of intracellular reactive oxygen species, PLoS One 5 (2010).
[16] L. Goitre, E. De Luca, S. Braggion, E. Trapani, M. Guglielmotto, F. Biasi, M. Forni, A. Moglia, L. Trabalzini, S.F. Retta, KRIT1 loss of function causes a ROS-dependent upregulation of c-Jun, Free Radic. Biol. Med. 68 (2014) 134–147.
[17] L. Goitre, P.V. DiStefano, A. Moglia, N. Nobiletti, E. Baldini, L. Trabalzini, J. Keubel, E. Trapani, V.V. Shuvaev, V.R. Muzykantov, I.H. Sarelius, S.F. Retta, A.J. Glading, Up-regulation of NADPH oxidase-mediated redox signaling contributes to the loss of barrier function in KRIT1 deficient endothelium, Sci. Rep. 7 (2017) 8296.
[18] S. Marchi, M. Corricelli, E. Trapani, L. Bravi, A. Pittaro, S. Delle Monache, L. Ferroni, S. Patergnani, S. Missiroli, L. Goitre, L. Trabalzini, A. Rimessi, C. Giorgi, B. Zavan, P. Cassoni, E. Dejana, S.F. Retta, P. Pinton, Defective autophagy is a key feature of cerebral cavernous malformations, Embo Mol. Med. 7 (2015) 1403–1417.
[19] S. Marchi, S.F. Retta, P. Pinton, Cellular processes underlying cerebral cavernous malformations: autophagy as another point of view, Autophagy 12 (2016) 424–425.
[20] S. Marchi, E. Trapani, M. Corricelli, L. Goitre, P. Pinton, S.F. Retta, Beyond multiple mechanisms and a unique drug: defective autophagy as pivotal player in cerebral cavernous malformation pathogenesis and implications for targeted therapies, Rare Dis. 4 (2016) e1142640.
[21] S.F. Retta, A.J. Glading, Oxidative stress and inflammation in cerebral cavernous malformation disease pathogenesis: two sides of the same coin, Int. J. Biochem. Cell Biol. 81 (2016) 254–270.
[22] A. Moglia, L. Goitre, S. Gianoglio, E. Baldini, E. Trapani, A. Genre, A. Scattina, G. Dondo, L. Trabalzini, J. Beekwilder, S.F. Retta, Evaluation of the bioactive properties of avenanthramide analogs produced in recombinant yeast, Biofactors 41 (2015) 15–27.
[23] J.W. Kaspar, S.K. Niture, A.K. Jaiswal, Nrf2:INrf2 (Keap1) signaling in oxidative stress, Free Radic. Biol. Med. 47 (2009) 1304–1309.
[24] T.W. Kensler, N. Wakabayashi, S. Biswal, Cell survival responses to environmental stresses via the Keap1-Nrf2-ARE pathway, Annu Rev. Pharmacol. Toxicol. 47 (2007) 89–116.
[25] G.E. Mann, Nrf2-mediated redox signalling in vascular health and disease, Free Radic. Biol. Med. 75 (Suppl 1) (2014) (S1).
[26] S. Jiang, Y. Yang, T. Li, Z. Ma, W. Hu, C. Deng, C. Fan, J. Lv, Y. Sun, W. Yi, An overview of the mechanisms and novel roles of Nrf2 in cardiovascular diseases, Expert Opin. Ther. Targets 20 (2016) 1413–1424.
[27] A. Alfieri, S. Srivastava, R.C. Siow, D. Cash, M. Modo, M.R. Duchen, P.A. Fraser, S.C. Williams, G.E. Mann, Sulforaphane preconditioning of the Nrf2/HO-1 defense pathway protects the cerebral vasculature against blood-brain barrier disruption and neurological deficits in stroke, Free Radic. Biol. Med. 65 (2013) 1012–1022.
[28] A. Alfieri, S. Srivastava, R.C. Siow, M. Modo, P.A. Fraser, G.E. Mann, Targeting the Nrf2-Keap1 antioxidant defence pathway for neurovascular protection in stroke, J. Physiol. 589 (2011) 4125–4136.
[29] M. Xue, N. Rabbani, H. Momiji, P. Imbasi, M.M. Anwar, N. Kitteringham, B.K. Park, T. Souma, T. Moriguchi, M. Yamamoto, P.J. Thornalley, Transcriptional control of glyoxalase 1 by Nrf2 provides a stress-responsive defence against dicarbonyl glycation, Biochem. J. 443 (2012) 213–222.
[30] P.J. Thornalley, Glyoxalase I–structure, function and a critical role in the enzymatic defence against glycation, Biochem. Soc. Trans. 31 (2003) 1343–1348.
[31] P.J. Thornalley, Protein and nucleotide damage by glyoxal and methylglyoxal in physiological systems–role in ageing and disease, Drug Metabol. Drug Interact. 23 (2008) 125–150.

[32] J. Zeng, M.J. Davies, Evidence for the formation of adducts and S-(carboxymethyl) cysteine on reaction of alpha-dicarbonyl compounds with thiol groups on amino acids, peptides, and proteins, Chem. Res. Toxicol. 18 (2005) 1232–1241.
[33] N. Nass, K. Vogel, B. Hofmann, P. Presek, R.E. Silber, A. Simm, Glycation of PDGF results in decreased biological activity, Int. J. Biochem. Cell Biol. 42 (2010) 749–754.
[34] S.B. Bansode, A.D. Chougale, R.S. Joshi, A.P. Giri, S.L. Bodhankar, A.M. Harsulkar, M.J. Kulkarni, Proteomic analysis of protease resistant proteins in the diabetic rat kidney, Mol. Cell Proteom. 12 (2013) 228–236.
[35] P. Gillery, J.C. Monboisse, F.X. Maquart, J.P. Borel, Glycation of proteins as a source of superoxide, Diabetes Metab. 14 (1988) 25–30.
[36] K. Nowotny, T. Jung, A. Hohn, D. Weber, T. Grune, Advanced glycation end products and oxidative stress in type 2 diabetes mellitus, Biomolecules 5 (2015) 194–222.
[37] C. Antognelli, A. Gambelunghe, G. Muzi, V.N. Talesa, Peroxynitrite-mediated glyoxalase I epigenetic inhibition drives apoptosis in airway epithelial cells exposed to crystalline silica via a novel mechanism involving argpyrimidine-modified Hsp70, JNK, and NF-kappaB, Free Radic. Biol. Med. 84 (2015) 128–141.
[38] C. Antognelli, A. Gambelunghe, G. Muzi, V.N. Talesa, Glyoxalase I drives epithelial-to-mesenchymal transition via argpyrimidine-modified Hsp70, miR-21 and SMAD signalling in human bronchial cells BEAS-2B chronically exposed to crystalline silica Min-U-Sil 5: transformation into a neoplastic-like phenotype, Free Radic. Biol. Med. 92 (2016) 110–125.
[39] J. Kim, N.H. Kim, E. Sohn, C.S. Kim, J.S. Kim, Methylglyoxal induces cellular damage by increasing argpyrimidine accumulation and oxidative DNA damage in human lens epithelial cells, Biochem. Biophys. Res. Commun. 391 (2010) 346–351.
[40] J. Kim, O.S. Kim, C.S. Kim, E. Sohn, K. Jo, J.S. Kim, Accumulation of argpyrimidine, a methylglyoxal-derived advanced glycation end product, increases apoptosis of lens epithelial cells both in vitro and in vivo, Exp. Mol. Med. 44 (2012) 167–175.
[41] K.M. Kim, Y.S. Kim, D.H. Jung, J. Lee, J.S. Kim, Increased glyoxalase I levels inhibit accumulation of oxidative stress and an advanced glycation end product in mouse mesangial cells cultured in high glucose, Exp. Cell Res. 318 (2012) 152–159.
[42] C. Antognelli, A. Gambelunghe, V.N. Talesa, G. Muzi, Reactive oxygen species induce apoptosis in bronchial epithelial BEAS-2B cells by inhibiting the antiglycation glyoxalase I defence: involvement of superoxide anion, hydrogen peroxide and NF-kappa B, Apoptosis 19 (2014) 102–116.
[43] H. Sakamoto, T. Mashima, K. Yamamoto, T. Tsuruo, Modulation of heat-shock protein 27 (Hsp27) anti-apoptotic activity by methylglyoxal modification, J. Biol. Chem. 277 (2002) 45770–45775.
[44] C.G. Schalkwijk, J. van Bezu, R.C. van der Schors, K. Uchida, C.D.A. Stehouwer, V.W.M. van Hinsbergh, Heat-shock protein 27 is a major methylglyoxal-modified protein in endothelial cells, FEBS Lett. 580 (2006) 1565.
[45] N. Sreejayan, X. Yang, K. Palanichamy, K. Dolence, J. Ren, Antioxidant properties of argpyrimidine, Eur. J. Pharmacol. 593 (2008) 30–35.
[46] A. Jo-Watanabe, T. Ohse, H. Nishimatsu, M. Takahashi, Y. Ikeda, T. Wada, J. Shirakawa, R. Nagai, T. Miyata, T. Nagano, Y. Hirata, R. Inagi, M. Nangaku, Glyoxalase I reduces glycative and oxidative stress and prevents age-related endothelial dysfunction through modulation of endothelial nitric oxide synthase phosphorylation, Aging Cell 13 (2014) 519–528.
[47] W. Li, R.E. Maloney, M.L. Circu, J.S. Alexander, T.Y. Aw, Acute carbonyl stress induces occludin glycation and brain microvascular endothelial barrier dysfunction: role for glutathione-dependent metabolism of methylglyoxal, Free Radic. Biol. Med. 54 (2013) 51–61.
[48] M. Wortmann, A.S. Peters, M. Hakimi, D. Bockler, S. Dihlmann, Glyoxalase I (Glo1) and its metabolites in vascular disease, Biochem. Soc. Trans. 42 (2014) 528–533.
[49] C. Antognelli, E. Trapani, S. Delle Monache, A. Perrelli, C. Fornelli, F. Retta, P. Cassoni, V.N. Talesa, S.F. Retta, Data in support of sustained upregulation of adaptive redox homeostasis mechanisms caused by KRIT1 loss-of-function, Data Brief (2017) (co-submitted for publication).
[50] K.J. Livak, T.D. Schmittgen, Analysis of relative gene expression data using real-time quantitative PCR and the 2(T)(-Delta Delta C) method, Methods 25 (2001) 402–408.
[51] C. Antognelli, L. Mezzasoma, K. Fettucciari, E. Mearini, V.N. Talesa, Role of glyoxalase I in the proliferation and apoptosis control of human LNCaP and PC3 prostate cancer cells, Prostate 73 (2013) 121–132.
[52] B. Mannervik, A.C. Aronsson, E. Marmstal, G. Tibbelin, Glyoxalase I (rat liver), Methods Enzymol. 77 (1981) 297–301.
[53] H.J. Forman, O. Augusto, R. Brigelius-Flohe, P.A. Dennery, B. Kalyanaraman, H. Ischiropoulos, G.E. Mann, R. Radi, L.J. Roberts 2nd, J. Vina, K.J. Davies, Even free radicals should follow some rules: a guide to free radical research terminology and methodology, Free Radic. Biol. Med. 78 (2015) 233–235.
[54] P. Dmitriev, Y. Bou Saada, C. Dib, E. Ansseau, A. Barat, A. Hamade, P. Dessen, T. Robert, V. Lazar, R.A.N. Louzada, C. Dupuy, V. Zakharova, G. Carnac, M. Lipinski, Y.S. Vassetzky, DUX4-induced constitutive DNA damage and oxidative stress contribute to aberrant differentiation of myoblasts from FSHD patients, Free Radic. Biol. Med. 99 (2016) 244–258.
[55] C. Antognelli, I. Palumbo, C. Aristei, V.N. Talesa, Glyoxalase I inhibition induces apoptosis in irradiated MCF-7 cells via a novel mechanism involving Hsp27, p53 and NF-kappaB, Br. J. Cancer 111 (2014) 395–406.
[56] P.V. DiStefano, J.M. Kuebel, I.H. Sarelius, A.J. Glading, KRIT1 protein depletion modifies endothelial cell behavior via increased vascular endothelial growth factor (VEGF) signaling, J. Biol. Chem. 289 (2014) 33054–33065.
[57] M. Moglianetti, E. De Luca, D. Pedone, R. Marotta, T. Catelani, B. Sartori, H. Amenitsch, S.F. Retta, P.P. Pompa, Platinum nanozymes recover cellular ROS homeostasis in an oxidative stress-mediated disease model, Nanoscale 8 (2016) 3739–3752.
[58] N. Miyazawa, M. Abe, T. Souma, M. Tanemoto, T. Abe, M. Nakayama, S. Ito, Methylglyoxal augments intracellular oxidative stress in human aortic endothelial cells, Free Radic. Res. 44 (2010) 101–107.
[59] T. Oba, R. Tatsunami, K. Sato, K. Takahashi, Z. Hao, Y. Tampo, Methylglyoxal has deleterious effects on thioredoxin in human aortic endothelial cells, Environ. Toxicol. Pharmacol. 34 (2012) 117–126.
[60] A.O. Oyewole, M.C. Wilmot, M. Fowler, M.A. Birch-Machin, Comparing the effects of mitochondrial targeted and localized antioxidants with cellular antioxidants in human skin cells exposed to UVA and hydrogen peroxide, FASEB J. 28 (2014) 485–494.
[61] H.K. Bryan, A. Olayanju, C.E. Goldring, B.K. Park, The Nrf2 cell defence pathway: Keap1-dependent and -independent mechanisms of regulation, Biochem. Pharmacol. 85 (2013) 705–717.
[62] C. Espinosa-Diez, V. Miguel, D. Mennerich, T. Kietzmann, P. Sanchez-Perez, S. Cadenas, S. Lamas, Antioxidant responses and cellular adjustments to oxidative stress, Redox Biol. 6 (2015) 183–197.
[63] A. Loboda, M. Damulewicz, E. Pyza, A. Jozkowicz, J. Dulak, Role of Nrf2/HO-1 system in development, oxidative stress response and diseases: an evolutionarily conserved mechanism, Cell Mol. Life Sci. (2016).
[64] S.R. McSweeney, E. Warabi, R.C. Siow, Nrf2 as an endothelial mechanosensitive transcription factor: going with the flow, Hypertension 67 (2016) 20–29.
[65] D. Morse, L. Lin, A.M. Choi, S.W. Ryter, Heme oxygenase-1, a critical arbitrator of cell death pathways in lung injury and disease, Free Radic. Biol. Med. 47 (2009) 1–12.
[66] Z. Zhou, A.T. Tang, W.Y. Wong, S. Bamezai, L.M. Goddard, R. Shenkar, S. Zhou, J. Yang, A.C. Wright, M. Foley, J.S. Arthur, K.J. Whitehead, I.A. Awad, D.Y. Li, X. Zheng, M.L. Kahn, Cerebral cavernous malformations arise from endothelial gain of MEKK3-KLF2/4 signalling, Nature 532 (2016) 122–126.
[67] G. Filomeni, D. De Zio, F. Cecconi, Oxidative stress and autophagy: the clash between damage and metabolic needs, Cell Death Differ. 22 (2015) 377–388.
[68] S. Giordano, V. Darley-Usmar, J. Zhang, Autophagy as an essential cellular antioxidant pathway in neurodegenerative disease, Redox Biol. 2 (2014) 82–90.
[69] T. Jiang, B. Harder, M. Rojo de la Vega, P.K. Wong, E. Chapman, D.D. Zhang, P62 links autophagy and Nrf2 signaling, Free Radic. Biol. Med. 88 (2015) 199–204.
[70] A. Lau, X.J. Wang, F. Zhao, N.F. Villeneuve, T. Wu, T. Jiang, Z. Sun, E. White, D.D. Zhang, A noncanonical mechanism of Nrf2 activation by autophagy deficiency: direct interaction between Keap1 and p62, Mol. Cell Biol. 30 (2010) 3275–3285.
[71] S. Srivastava, A. Alfieri, R.C. Siow, G.E. Mann, P.A. Fraser, Temporal and spatial distribution of Nrf2 in rat brain following stroke: quantification of nuclear to cytoplasmic Nrf2 content using a novel immunohistochemical technique, J. Physiol. 591 (2013) 3525–3538.
[72] R. Arya, M. Mallik, S.C. Lakhotia, Heat shock genes - integrating cell survival and death, J. Biosci. 32 (2007) 595–610.
[73] H.M. Beere, Death versus survival: functional interaction between the apoptotic and stress-inducible heat shock protein pathways, J. Clin. Investig. 115 (2005) 2633–2639.
[74] G. Wettstein, P.S. Bellaye, O. Micheau, P. Bonniaud, Small heat shock proteins and the cytoskeleton: an essential interplay for cell integrity? Int. J. Biochem. Cell Biol. 44 (2012) 1680–1686.
[75] S.B. Nadin, F.D. Cuello-Carrion, M.L. Sottile, D.R. Ciocca, L.M. Vargas-Roig, Effects of hyperthermia on Hsp27 (HSPB1), Hsp72 (HSPA1A) and DNA repair proteins hMLH1 and hMSH2 in human colorectal cancer hMLH1-deficient and hMLH1-proficient cell lines, Int. J. Hyperth. 28 (2012) 191–201.
[76] M.K. Kenny, F. Mendez, M. Sandigursky, R.P. Kureekattil, J.D. Goldman, W.A. Franklin, R. Bases, Heat shock protein 70 binds to human apurinic/apyrimidinic endonuclease and stimulates endonuclease activity at abasic sites, J. Biol. Chem. 276 (2001) 9532–9536.
[77] F. Mendez, E. Kozin, R. Bases, Heat shock protein 70 stimulation of the deoxyribonucleic acid base excision repair enzyme polymerase beta, Cell Stress Chaperon. 8 (2003) 153–161.
[78] T. Oya-Ito, B.F. Liu, R.H. Nagaraj, Effect of methylglyoxal modification and phosphorylation on the chaperone and anti-apoptotic properties of heat shock protein 27, J. Cell Biochem. 99 (2006) 279–291.
[79] J.W. van Heijst, H.W. Niessen, R.J. Musters, V.W. van Hinsbergh, K. Hoekman, C.G. Schalkwijk, Argpyrimidine-modified Heat shock protein 27 in human non-small cell lung cancer: a possible mechanism for evasion of apoptosis, Cancer Lett. 241 (2006) 309–319.
[80] C.M. Cabello, W.B. Bair 3rd, A.S. Bause, G.T. Wondrak, Antimelanoma activity of the redox dye DCPIP (2,6-dichlorophenolindophenol) is antagonized by NQO1, Biochem. Pharmacol. 78 (2009) 344–354.
[81] M. Madesh, G. Hajnoczky, VDAC-dependent permeabilization of the outer mitochondrial membrane by superoxide induces rapid and massive cytochrome c release, J. Cell Biol. 155 (2001) 1003–1015.
[82] S.H. Kaufmann, M.O. Hengartner, Programmed cell death: alive and well in the new millennium, Trends Cell Biol. 11 (2001) 526–534.
[83] G. Boulday, N. Rudini, L. Maddaluno, A. Blecon, M. Arnould, A. Gaudric, F. Chapon, R.H. Adams, E. Dejana, E. Tournier-Lasserve, Developmental timing of CCM2 loss influences cerebral cavernous malformations in mice, J. Exp. Med. 208 (2011) 1835–1847.
[84] A.C. Chan, S.G. Drakos, O.E. Ruiz, A.C. Smith, C.C. Gibson, J. Ling, S.F. Passi, A.N. Stratman, A. Sacharidou, M.P. Revelo, A.H. Grossmann, N.A. Diakos,

G.E. Davis, M.M. Metzstein, K.J. Whitehead, D.Y. Li, Mutations in 2 distinct genetic pathways result in cerebral cavernous malformations in mice, J. Clin. Investig. 121 (2011) 1871–1881.
[85] M. Komatsu, Y. Ichimura, Selective autophagy regulates various cellular functions, Genes Cells 15 (2010) 923–933.
[86] S.N. Zucker, E.E. Fink, A. Bagati, S. Mannava, A. Bianchi-Smiraglia, P.N. Bogner, J.A. Wawrzyniak, C. Foley, K.I. Leonova, M.J. Grimm, K. Moparthy, Y. Ionov, J. Wang, S. Liu, S. Sexton, E.S. Kandel, A.V. Bakin, Y. Zhang, N. Kaminski, B.H. Segal, M.A. Nikiforov, Nrf2 amplifies oxidative stress via induction of Klf9, Mol. Cell 53 (2014) 916–928.
[87] R.J. Dekker, R.A. Boon, M.G. Rondaij, A. Kragt, O.L. Volger, Y.W. Elderkamp, J.C. Meijers, J. Voorberg, H. Pannekoek, A.J. Horrevoets, KLF2 provokes a gene expression pattern that establishes functional quiescent differentiation of the endothelium, Blood 107 (2006) 4354–4363.
[88] M. Dodson, M. Redmann, N.S. Rajasekaran, V. Darley-Usmar, J. Zhang, KEAP1-NRF2 signalling and autophagy in protection against oxidative and reductive proteotoxicity, Biochem. J. 469 (2015) 347–355.
[89] K.M. Holmstrom, T. Finkel, Cellular mechanisms and physiological consequences of redox-dependent signalling, Nat. Rev. Mol. Cell Biol. 15 (2014) 411–421.
[90] S. Kovac, P.R. Angelova, K.M. Holmstrom, Y. Zhang, A.T. Dinkova-Kostova, A.Y. Abramov, Nrf2 regulates ROS production by mitochondria and NADPH oxidase, Biochim. Biophys. Acta 1850 (2015) 794–801.
[91] R. Howden, Nrf2 and cardiovascular defense, Oxid. Med. Cell Longev. 2013 (2013) 104308.
[92] R.C. Siow, G.E. Mann, Dietary isoflavones and vascular protection: activation of cellular antioxidant defenses by SERMs or hormesis? Mol. Asp. Med. 31 (2010) 468–477.
[93] N. Wakabayashi, K. Itoh, J. Wakabayashi, H. Motohashi, S. Noda, S. Takahashi, S. Imakado, T. Kotsuji, F. Otsuka, D.R. Roop, T. Harada, J.D. Engel, M. Yamamoto, Keap1-null mutation leads to postnatal lethality due to constitutive Nrf2 activation, Nat. Genet. 35 (2003) 238–245.
[94] L.E. Tebay, H. Robertson, S.T. Durant, S.R. Vitale, T.M. Penning, A.T. Dinkova-Kostova, J.D. Hayes, Mechanisms of activation of the transcription factor Nrf2 by redox stressors, nutrient cues, and energy status and the pathways through which it attenuates degenerative disease, Free Radic. Biol. Med. 88 (2015) 108–146.
[95] X. Yuan, C. Xu, Z. Pan, Y.S. Keum, J.H. Kim, G. Shen, S. Yu, K.T. Oo, J. Ma, A.N. Kong, Butylated hydroxyanisole regulates ARE-mediated gene expression via Nrf2 coupled with ERK and JNK signaling pathway in HepG2 cells, Mol. Carcinog. 45 (2006) 841–850.
[96] K. Taguchi, N. Fujikawa, M. Komatsu, T. Ishii, M. Unno, T. Akaike, H. Motohashi, M. Yamamoto, Keap1 degradation by autophagy for the maintenance of redox homeostasis, Proc. Natl. Acad. Sci. U.S.A. 109 (2012) 13561–13566.
[97] M. He, M. Nitti, S. Piras, A.L. Furfaro, N. Traverso, M.A. Pronzato, G.E. Mann, Heme oxygenase-1-derived bilirubin protects endothelial cells against high glucose-induced damage, Free Radic. Biol. Med. 89 (2015) 91–98.
[98] E. Marcantoni, L. Di Francesco, M. Dovizio, A. Bruno, P. Patrignani, Novel insights into the vasoprotective role of heme oxygenase-1, Int. J. Hypertens. 2012 (2012) 127910.
[99] E. Barone, F. Di Domenico, C. Mancuso, D.A. Butterfield, The Janus face of the heme oxygenase/biliverdin reductase system in Alzheimer disease: it's time for reconciliation, Neurobiol. Dis. 62 (2014) 144–159.
[100] C. Mancuso, E. Barone, The heme oxygenase/biliverdin reductase pathway in drug research and development, Curr. Drug Metab. 10 (2009) 579–594.
[101] M. Brownlee, The pathobiology of diabetic complications: a unifying mechanism, Diabetes 54 (2005) 1615–1625.
[102] W. Nomura, Y. Inoue, Methylglyoxal activates the target of rapamycin complex 2-protein kinase C signaling pathway in Saccharomyces cerevisiae, Mol. Cell Biol. 35 (2015) 1269–1280.
[103] B. Stratmann, B. Engelbrecht, B.C. Espelage, N. Klusmeier, J. Tiemann, T. Gawlowski, Y. Mattern, M. Eisenacher, H.E. Meyer, N. Rabbani, P.J. Thornalley, D. Tschoepe, G. Poschmann, K. Stuhler, Glyoxalase 1-knockdown in human aortic endothelial cells - effect on the proteome and endothelial function estimates, Sci. Rep. 6 (2016) 37737.
[104] M.G. Distler, N. Gorfinkle, L.A. Papale, G.E. Wuenschell, J. Termini, A. Escayg, M.R. Winawer, A.A. Palmer, Glyoxalase 1 and its substrate methylglyoxal are novel regulators of seizure susceptibility, Epilepsia 54 (2013) 649–657.
[105] A.S. Cheng, Y.H. Cheng, C.H. Chiou, T.L. Chang, Resveratrol upregulates Nrf2 expression to attenuate methylglyoxal-induced insulin resistance in Hep G2 cells, J. Agric. Food Chem. 60 (2012) 9180–9187.
[106] Y. Gao, C. Liu, G. Wan, X. Wang, X. Cheng, Y. Ou, Phycocyanin prevents methylglyoxal-induced mitochondrial-dependent apoptosis in INS-1 cells by Nrf2, Food Funct. 7 (2016) 1129–1137.
[107] R. Chovatiya, R. Medzhitov, Stress, inflammation, and defense of homeostasis, Mol. Cell 54 (2014) 281–288.
[108] K.J. Davies, Adaptive homeostasis, Mol. Asp. Med. 49 (2016) 1–7.